JOURNAL OF MATERIALS SCIENCE 11 (1976) 1542–1566

Review

Steady-state creep of single-phase crystalline matter at high temperature

S. TAKEUCHI*, A. S. ARGON
Massaschusetts Institute of Technology, Cambridge, Mass., USA

Over the past 15 years important advances have been made in the experimental study of the microstructural changes occurring during the non-linear steady-state creep of single phase crystalline matter at elevated temperatures. Curiously, although the results of these painstaking studies have gone a long way toward elucidating the mechanism of this phenomenon, they have been largely ignored in favour of some simple dislocation mechanisms that are not only inconsistent with these observations, but are also unable to describe correctly the known phenomenology. This review concentrates primarily on the recent experiments on microstructural alterations occurring during creep; however, it also surveys the many mechanistic models that attempt to describe this phenomenon, and finds them all deficient.

1. Introduction

High temperature creep of crystalline matter has received continued interest for many decades both from the practical point of view, and also from the point of the mechanism of inelastic deformation at high temperature. The mechanism of slow deformation above half the melting point has aspects essentially different from that at low temperature: the rate of deformation at high temperature is primarily controlled by atomic diffusion, which is absent at low temperature. After the accumulation of a large number of creep experiments on various kinds of crystalline materials, the phenomenological and microstructural descriptions of high temperature creep seem to be nearly complete. Many theoretical models, of either phenomenological nature or based on dislocation theory, have been proposed for the creep mechanism at high temperature. The present situation, however, is still far from a complete understanding of all the experimental observations.

In recent years, considerable progress has been made in the direct observation of changes in microstructure in creeping materials by transmission electron microscopy, and the etch-pit method. Experiments, on creep transients, in particular the so-called "dip-tests", have contributed additional understanding. Therefore, although several recent review articles on this subject exist [1–14], it seems worthwhile to resurvey this field mainly concentrating our attention on the above experiments.

Materials to be dealt with will be limited primarily to single phase crystalline materials including metals, alloys and ceramics. The phenomenon to be treated is that which has initially been studied by Andrade in 1911 and which is currently referred to as "power-law" creep†, where the creep deformation is due mainly to the glide and climb motion of dislocations

*On leave from The Institute for Solid State Physics, The University of Tokyo, during 1974–1975.

†Although other creep phenomena of far less technological importance are currently named after their discoverers, curiously, this most important component of steady-state creep is not named after Andrade on the ground that this would imply to some only the transient phase of this creep phenomenon, having roughly a $t^{1/3}$ time law. In keeping with the increasing usage of the terminology of "Andradean viscosity" for this phenomenon in the field of geology, we propose that the uninspiring terminology of "power-law creep" be dropped in favour of "Andradean creep".

controlled by diffusion. Creep phenomena occur in at very high temperature, at very low stress and the behaviour of the very fine-grained materials, exhibiting creep phenonomena classified as Nabarro–Herring creep [15, 16], Coble creep [17], Harper–Dorn creep [18], as well as the phenomenon of superplasticity (for a review see [19]), will not be considered.

In this review, after summarizing briefly the phenomenological descriptions of the creep process, the qualitative and quantiative aspects of the changes in microstructure will be described, then the results of experiments on creep transients will be summarized, and finally current theories on the mechanism of steady-state creep will be discussed in the light of these experimental facts. The effect of grain size on the creep rate has been reviewed previously [6, 9, 14] and it has been shown that as far as the steady-state is concerned the creep rate is not much influenced by grain size if the latter is not too small [9, 14, 20]. Although the contribution of grain-boundary sliding to the creep strain [20–23], and the dislocation structures resulting from the grain-boundary sliding induced inhomogeneous deformation in polycrystals [24–27] have long been recognized, there is no essential difference between polycrystals and single crystals with regard to the controlling mechanism of steady-state creep. Thus, no special attention will be paid to the role of the grain boundary in the creep microstructure. Recent theoretical developments in grain-boundary sliding accommodated by diffusion and by plastic flow inside the grain governed by power law creep will be briefly reviewed in Section 5.

2. Creep equations

2.1. The creep curve

Typical creep curves of annealed crystalline materials are composed of four stages, i.e. instantaneous strain, transient or primary creep, steady-state or secondary creep, and tertiary creep that is usually connected with fracture which will not be the subject of this review. More than a half-century ago, Andrade analysed the creep curves of metals and showed that the creep strain ϵ is proportional to time to the $\frac{1}{3}$ power (i.e. $\epsilon \propto t^{1/3}$) at the initial stage [28]. The creep curve up to the end of steady-state creep can often be expressed by the following equation (called sometimes the Cottrell–Aytekin equation [29]).

$$\epsilon = \epsilon_0 + at^{1/3} + \dot{\epsilon}_s t . \quad (1)$$

Here, ϵ_0 is the instantaneous strain, a is a constant and $\dot{\epsilon}_s$ is an asymptotic creep rate as $t \to \infty$. So far, many types of empirical equations of transient creep have been proposed besides Equation 1 (see [30]), but as shown by Conway and Mullikin different equations can accurately represent a given set of data by choosing the different parameters appropriately; consequently, the degree of fit obtained by different functional forms cannot be used to assess relative merit, and differences cannot easily be discerned experimentally [30]. Among these different functional forms the equation originally proposed by McVetty [31] is noteworthy,

$$\epsilon = \epsilon_0 + \epsilon_T \left[1 - \exp\left(-\frac{t}{t_r}\right)\right] + \dot{\epsilon}_s t . \quad (2)$$

Here, ϵ_T corresponds to the asymptotic transient strain component and t_r is a time constant. Because of extensive use of this equation by Garofalo [6], it is often called the Garofalo equation. As Webster *et al.* showed [32], the above equation can be derived from the differential equation for first order kinetics, i.e.

$$\frac{d\dot{\epsilon}}{dt} = -\frac{\dot{\epsilon} - \dot{\epsilon}_s}{t_r} . \quad (3)$$

Although the physical meaning of the relaxation time, t_r, is not at all clear, Equation 3 has a natural form for transient creep. Another operational advantage of Equation 2 over Equation 1 is [32], that the former can define a finite value of initial strain-rate $\dot{\epsilon}_i \equiv (d\epsilon/dt)_{t=0} = \dot{\epsilon}_s + \epsilon_T/t_r$, in contrast to Equation 1: this corresponds to the experimental observation of this quantity. As first demonstrated by Garofalo *et al.* for stainless steel [33], $\dot{\epsilon}_i$ has often been reported to be proportional to $\dot{\epsilon}_s$ [32–35], which suggests that, not surprisingly, the kinetics of transient creep and steady-state creep are governed by the same mechanism. From this relation, the asymptotic strain ϵ_T is related to $\dot{\epsilon}_s$ by the equation,

$$\frac{\epsilon_T}{t_r} \propto \dot{\epsilon}_s . \quad (4)$$

Webster *et al.* [32] have also shown for some metals the proportionality between $1/t_r$ and $\dot{\epsilon}_s$, which in turn leads to constant ϵ_T. In this case all the creep curves are to be fitted together by use of a normalized time scale of $\dot{\epsilon}_s t$.

Li derived a transient creep equation from a dislocation mechanism [36]. He obtained a com-

prehensive functional form starting from the time equation of mobile dislocation density proposed by Johnston and Gilman [37], but the general applicability of the basic assumptions is questionable.

It should be noted that in some cases, mainly in alloys under low stress, the transient creep curve is significantly different from that expressed by Equations 1 or 2. In such cases transient creep with gradual acceleration [38–41] and sigmoidal transient creep [42–45] has been observed. Menerzes *et al.* [43, 44] successfully analysed the sigmoidal creep curve of LiF single cyrstals according to the theory of Haasen *et al.* (see [46]), where the initial acceleration of the creep rate is attributed to the increase of mobile dislocation density and the deceleration at the later stage to work hardening due to multiplied dislocations. Similar arguments can be applied to other crystals. It is also known that the shape of the transient creep curve changes drastically with prior cold work; and sigmoidal curves are also obtained in pre-strained materials (see, e.g. [47]).

2.2. Steady-state creep equation

It has been established earlier that steady-state creep rate under the usual creep condition is best expressed as a function of temperature and stress by $\dot{\epsilon}_s \propto \sigma^n \exp(-Q_c/kT)$, where σ is the applied tensile stress, Q_c the activation energy of creep and kT has the usual meaning (e.g. [48]). Later theoretical justifications [49, 50] incorporated the elastic modulus, and also temperature into the pre-exponential factor [4]. Thus, the following type of empirical equation has been used most commonly [4, 10, 13, 14].

$$\dot{\epsilon}_s = A_0 \nu_D \left(\frac{\mu\Omega}{kT}\right)\left(\frac{\sigma}{\mu}\right)^n \exp\left(-\frac{Q_c}{kT}\right). \quad (5)$$

Here, μ is the shear modulus, ν_D the atomic frequency and Ω the atomic volume, A_0 and n are non-dimensional constants.

Garofalo proposed a stress dependence of the type $(\sinh B\sigma)^n$ (where B is a constant) which showed good agreement with experiments for some alloys over a wide range of stress [51]. The steady-state strain-rate $\dot{\epsilon}_s^{hw}$ under hot-working conditions has also been shown to be represented by the following equation over a wide stress range [52–54, 12].

$$\dot{\epsilon}_s^{hw} = A_0' (\sinh B\sigma)^n \exp\left(-\frac{Q}{kT}\right) \quad (6)$$

Here, A_0' and B are material constants. At low stress, Equation 6 is reduced to a form similar to Equation 5.

Another alternative expression is that based on the concept of the stress assisted thermally activated motion of dislocations [5, 7, 55–57] and is written as

$$\dot{\epsilon}_s = 2\dot{\epsilon}_0 \sinh\left(\frac{v^*\tau}{kT}\right) \exp\left(-\frac{Q}{kT}\right), \quad (7)$$

where $\dot{\epsilon}_0$ is a constant having dimensions of reciprocal time, τ the resolved shear stress, and v^* the activation volume which is in general a function of stress. When $v^*\tau/kT \gg 1$ is satisfied, Equation 7 is approximated by

$$\dot{\epsilon}_s = \epsilon_0 \exp\left(-\frac{Q - v^*\tau}{kT}\right). \quad (8)$$

Jonas introduced a back stress term in τ [58] to take account of internal stresses. Several researchers analysed their data to determine the activation area $A^*(=v^*/b)$ in the creep process [57–64] and the experimental values of A^* range between 10^2 and $10^3 b^2$. In the following equation of the type of Equation 5 is used simply because the majority of the experimental data is well represented by this equation, for which mechanistic models are also more readily obtainable.

2.2.1. Activation energy

Good agreement between the activation energy of steady-state creep rate and that of self diffusion has been shown for a number of materials (see reviews [5–8, 10, 13, 14, 65]). The correspondence between these two quantities has most clearly been demonstrated in the case of phase transitions [66, 67] including magnetic transition [56]. In this comparison, it has been pointed out that temperature dependence of μ in Equation 5 has to be taken into consideration in evaluating Q_c [68, 69]. The above correspondence excludes mechanisms in which the activation process does not involve self-diffusion.

Using the diffusion coefficient, D, Equation 5 is simplified as

$$\dot{\epsilon}_s = A\frac{\mu b D}{kT}\left(\frac{\sigma}{\mu}\right)^n, \quad (9)$$

where A and n are non-dimensional constants which can be considered as universal if no material constants other than μ, b, and D are involved in the mechanism of the creep process.

2.2.2. Stress exponent

A typical value of n for pure metals is 5. With the addition of solute elements, the value of n decreases rapidly and in the case of some solid solution alloys drops down to 3 [41, 70, 71] while in other solid solution alloys it remains high at a value around 5 (see [14]). Sherby and Burke [8] classified the former type of alloys as class I and the latter as class II*.

Cannon and Sherby found a correlation between the alloy type, and the size parameter of solute element and elastic modulus [73]. They rationalized this correlation on the assumption that creep is a series process involving the viscous glide motion of dislocations obeying a third power law of τ/μ and the climb motion of dislocations obeying a fifth power law of τ/μ; the creep rate being controlled by the slower of the two processes. From this argument, they anticipated that a transition from class II to class I behaviour occurs as the stress increases. This transition has, in fact, been reported to occur in some alloys [72, 74]. Recently, Mohamed and Langdon gave a more elaborate discussion of this problem along similar lines and showed that the behaviour of most of the alloys is consistent with the criterion they stated [72, 75]. In general, a large size misfit of solute atoms, a high concentration of solute, and high stacking fault energy tend to lead to class I behaviour.

2.2.3. Effect of stacking fault energy

The effect of stacking fault energy, γ, was first pointed out by Barrett and Sherby [76] for pure fcc metals, where, for the same σ/μ and D, $\dot{\epsilon}_s \propto \gamma^{3.5}$. Effect of the change in γ due to alloying on the creep rate has also been discussed [77–80]. For copper-base alloys, an alternative expression of $\dot{\epsilon}_s \propto \exp(k_1\gamma/\mu b)$ has been proposed, where k_1 is a constant [80]. Fig. 1 shows the relation between normalized creep rate (at $\sigma/\mu = 2 \times 10^{-4}$) and $\gamma/\mu b$ for twenty-five fcc metals and alloys compiled by Mohamed and Langdon [72]. The creep rate of 80% of all fcc metals and alloys is found to be well represented by substituting for A in equation 9

$$A = A'\left(\frac{\gamma}{\mu b}\right)^3, \qquad (10)$$

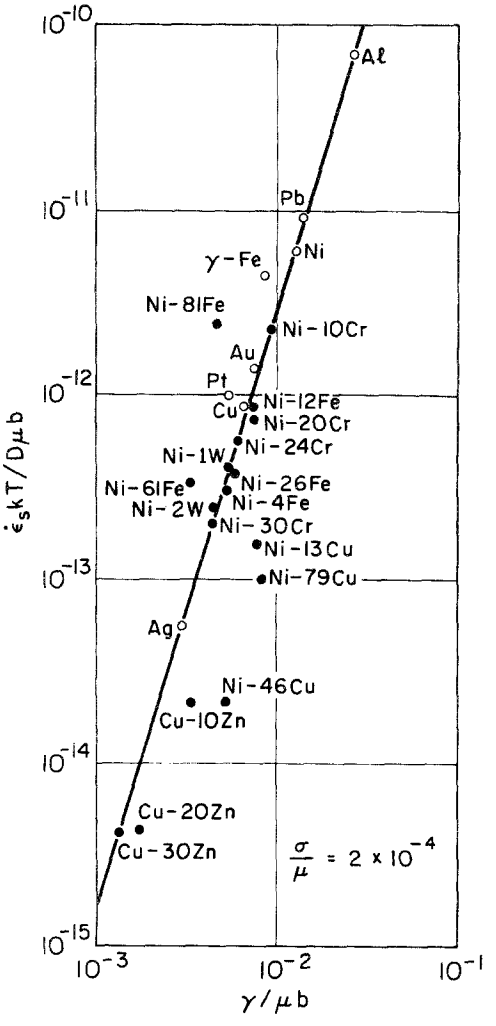

Figure 1 Relation between normalized creep rate at $\sigma/\mu = 2 \times 10^{-4}$ and normalized stacking fault energy for 25 fcc metals and alloys, (from [72]).

where A' is a new non-dimentional constant.

On the other hand, Bird *et al.* [14] noticed a systematic effect of the creep rate on the stress exponent for fcc metals, and correlated the value of n with the stacking fault energy assuming A to be a universal constant, i.e. n is a gradually increasing function of $\mu b/\gamma$. Considering the scatter of the experimental data, it cannot be easily decided which expression is more appropriate. It appears safe, however, to say that around the usual stress range of $\sigma/\mu \simeq 10^{-4}$, the temperature compensated creep rate, $\dot{\epsilon}_s kT/D\mu b$, tends to have larger values for fcc metals with larger stacking fault energy.

*In a recent paper [72], this classification of class I and class II has been reversed, but in this paper we follow the original definition of Sherby and Burke.

TABLE I Values of n and A in Equation 9 for various metals by Bird *et al.* [14]. Typical values for each case are shown in parentheses

Material	n	A
f c c metals	4.4–5.3 (5)	10^5–10^8 (10^7)
b c c metals	4–7 (5)	10^5–10^{15} (10^9)
h c p metals	4–6 (5)	10^3–10^8 (10^6)
Class II alloys	4.5–6 (5)	10^5–10^9 (10^6)
Class I alloys	3–4 (3.3)	10^{-2}–10^4 (10^1)

2.2.4. Values of constants

The most elaborate task of determing the constants A and n in Equation 9 for many materials has been performed by Mukherjee, Bird and Dorn [13, 14]. The extent of these values for various kinds of metals is listed in Table I.

For f c c metals, Bird *et al.* have shown that when an appropriate value of n for each metal is selected according to their n–γ diagram, all the creep data are well represented within a factor of two by setting $A = 2.5 \times 10^6$. This is in contrast to the expression of Equation 7 as mentioned above. On the other hand, for b c c metals n varies over a wide range even for the same material, but instead the whole experimental data fall in a relatively narrow region. Fig. 2 shows regions where data for different kinds of materials are included.

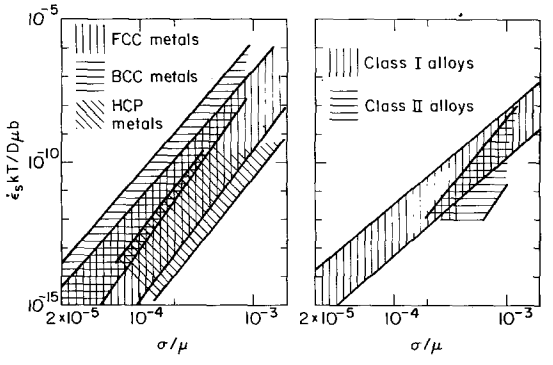

Figure 2 Regions of five types of metals in which creep data are included in $\dot{\epsilon}_s kT/D\mu b$ versus σ/μ plot (from [14]).

Not many data are available for ionic crystals. For poly-crystalline NaCl, KCl and LiF $n = 5$ to 6 and $A = 10^8$ to 10^{12} [81], and the data points fall in the b c c region. For MgO [82, 83], $n = 3.3$ and $A \approx 10$, and the data fits the behaviour of class I alloys.

3. Microstructures

Since the first observation of Jenkins and Mellor [84] on the fragmentation of grains during high temperature deformation, the most characteristic microstructure in crept materials has been referred to as "substructure", a term which has become frequently used since the investigations around 1950 [21, 85–92]. Substructures have been investigated by X-ray and/or light microscopy techniques until recent years, when transmission electron microscopy and the dislocation etch-pit technique have become available for the detailed and quantitative studies on microstructures in crept materials. Because of the limited resolving power of the earlier techniques, some of the quantitative estimates, e.g. for subgrain size or misorientation angle, obtained earlier, have been found at times to be erroneous [14]. However, the qualitative features of subgrain formation and its mechanism have been established at the beginning of the 1950s: these mechanisms of substructure formation are poligonization and kinking [27, 88, 91–95].

3.1. Surface observations

Coarse slip bands have been observed for various materials mainly at an early stage of creep strain and their average spacing has often been correlated with the reciprocal of the applied stress [92, 96]. McLean estimated contributions of coarse slip and grain-boundary sliding to the creep strain and found that about half of the total strain must be due to processes other than the above two [21]. He attributed this "missing creep" to fine slip. Another important feature is the formation of deformation bands, kink bands [89, 94, 95], and folds [97, 98]. Folding in grains is associated with grain-boundary sliding [98] and does not occur in single crystals.

Surface observations after repolishing and restraining specimens crept previously to the steady-state stage have been reported for Al [24, 99]; an example is shown in Fig. 3. Two facts are noteworthy: (1) no sharp slip lines are resolved, indicating homogeneous distribution of dislocation sources; (2) migration of subgrain boundaries takes place, the velocity of which, in a typical case, is such that for every increment of 0.05 strain the whole crystal is swept by sub-boundaries. The latter fact has not been properly appreciated in creep phenomena until the recent

Figure 3 A micrograph of an aluminium specimen deformed 20% at 10^{-5} sec^{-1} (~ 1.0 MN m^{-2}) in tension at 500° C, electropolished, followed by an incremental strain of 1.5% at 500° C, showing migration of subboundaries, bar $\equiv 200\,\mu m$, (from Exell and Warrington [99], courtesy of Taylor and Francis Ltd).

measurements by Exell and Warrington [99], although experiments on stress-induced small-angle boundary migration have been made earlier [100–103]. The main results of Exell and Warrington on Al are: (1) the velocity of a subgrain boundary, $v_{sb} \propto \sigma^n \exp(-Q_{sd}/kT)$, where $n \approx 3.5$, and Q_{sd} is the activation energy for self diffusion; (2) $v_{sb}/d = \text{const.}$ for constant $\dot{\epsilon}_s$, where d is the average subgrain size; and (3) the strain contribution due to the sub-boundary migration amounts to be about 25% of the total strain. Migration of sub-boundaries in creep has also been observed by means of X-ray topography [104] and by transmission electron microscopy [105].

3.2. Process of stable structure formation

As stated before, the creep substructure is quite heterogeneous in polycrystals, owing to the influence of grain boundaries. Even in single crystals, substructure formed during transient creep is also heterogeneous on the scale of light microscopy. The general features are: (1) at the initial stage, the dislocation structure is essentially the same as in low temperature deformation; (2) the dislocation structure is quite heterogeneous at the start of the transient stage, and sub-boundaries begin to form as straining continues at a decreasing rate, except in class I alloys; (3) the dislocation structure gradually changes to a stable and homogeneous one in steady-state creep. The subgrain size in steady-state creep is independent of grain size [106] and is generally a function only of stress.

Transmission electron microscopy is not an appropriate technique to investigate the overall change of dislocation structure, because of the relatively large scale of the inhomogeneity of the structure and also because the subgrain itself is larger than the foil thickness. The most suitable method for the study of dislocation arrangements in creep is the dislocation etch-pit method, which has been applied to Fe [107, 108], Fe–3% Si [25, 106, 109], Cu [110–112], Cu alloys [113], Mo [114], NaCl [115], MgO [116], and LiF [117, 118]. The results on Cu [110, 112] can be taken as typical for f c c single crystals, those on Mo [114] typical for b c c metals, and those on MgO [116] typical for ionic crystals. According to these results no essential differences in the change of dislocation structure during transient creep can be detected among different crystal structures.

Although a wide variety of dislocation structures depending upon stress and temperature have been reported [115, 119, 120], the following process of structure development seems to be the most typical. (1) At the initial stage, the dislocation structure is uniform, forming cells resembling those that develop in low temperature deformation [110]. (2) Deformation bands or kink bands begin to appear as the strain increases and parallel tilt boundaries form around them, having a spacing which increases away from the kink bands [110, 111]. In addition to these polygonized tilt walls which are perpendicular both to the slip direction and slip plane, sub-boundaries nearly parallel to the slip plane also form [109–112]; these are considered to be twist boundaries consisting of co-planar dislocations. In general, the former type of simple tilt boundaries predominate at the early stage [25, 95, 111, 112, 114–116, 121–124]. (3) During the transient stage, a heterogeneous dislocation structure develops, where regions with dense parallel subgrains and regions with coarse subgrains or with hardly any sub-boundaries at all are distributed alternately

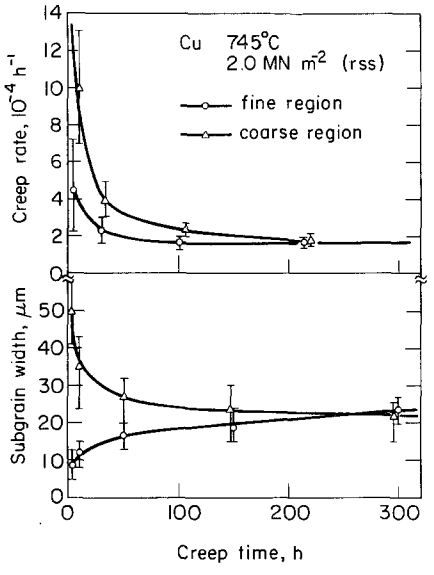

Figure 4 Changes in subgrain width and creep rate with creep time for two types of regions of substructure, fine subgrain region and coarse subgrain region, in a single crystal of Cu (from [112]).

[112, 114–116]. Hasegawa *et al.* measured the local strain-rate in the two regions in Cu and showed that it is higher in the coarse region than in the dense region [112]. (4) The dense substructure region gradually becomes coarser and the coarse region denser to establish a homogeneous substructure, and at the same time banded subgrains change to uniaxial ones. The changes in subgrain width and in the local strain-rate in the two regions measured for Cu single crystals are shown in Fig. 4 [112]. The above process of homogenization of dislocation structure is schematically depicted in Fig. 5. In the case of Mo single crystals investigated by Clauer *et al.* [114] no homogeneous dislocation structure was observed, which was consistent with the fact that no steady-state could be realized in this material before fracture [125].

Considering the high mobility of subgrain boundaries mentioned above, the coarsening of subgrains in the above process seems to take place mainly through the migration of sub-boundaries,

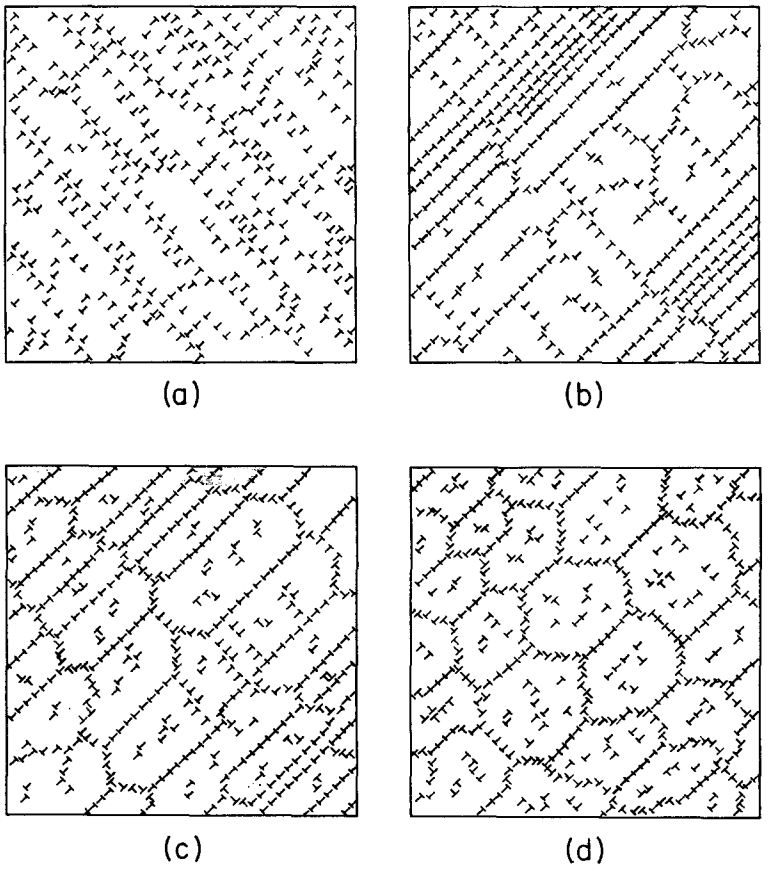

Figure 5 Schematic representation of creep structure in a single crystal at various stages; (a) after instantaneous strain, (b), (c) transient creep, (d) steady-state creep.

not by the coalescence of subgrains due to sub-boundary evaporation [126], as previously suggested by Gleiter [105] and Exell and Warrington [99]. Rather, the steady substructure is only steady on a time average and is realized through a dynamic balance between the rate of formation of new boundaries by decomposition into cells of higher energy dislocation structures produced during an increase of strain and that of annihilation due to impingement of sub-boundaries of opposite sign moving in the opposite directions [99, 127].

3.3. Dislocation structures

Direct observation of dislocations in crept materials by transmission electron microscopy has been reported in a number of papers (Al [127–133]; Al alloys [41, 134–138]; Cu [113, 122, 123, 139–143]; Cu alloys [44, 64, 113, 144, 145]; Fe [107, 108, 120, 146–148]; Fe alloys [149–153]; Ni [154, 155]; Mo [114]; stainless steel [119, 156–162]; Re [163]; W [164]; W alloy [165]; Zr [151]; MgO [83, 116, 124, 166]. Typical dislocation structures for bcc metals, fcc metals, ionic crystals and class I alloys are shown in Fig. 6.

General features of dislocation structures inside

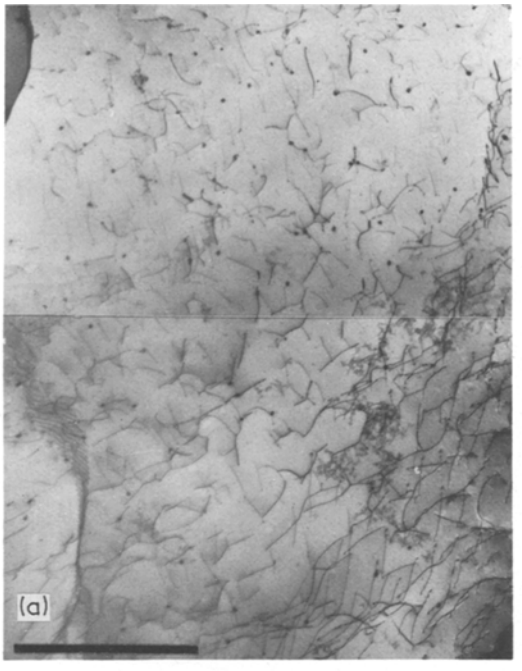

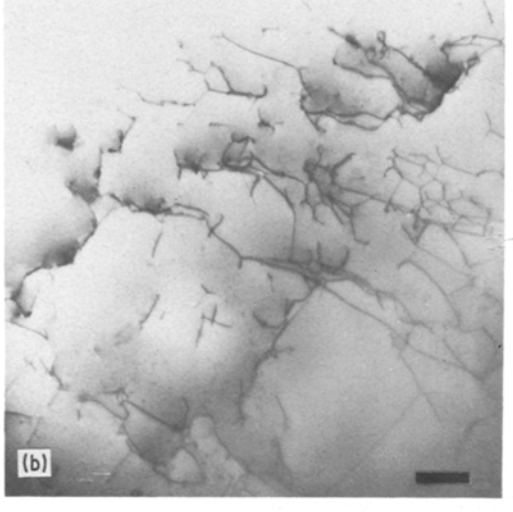

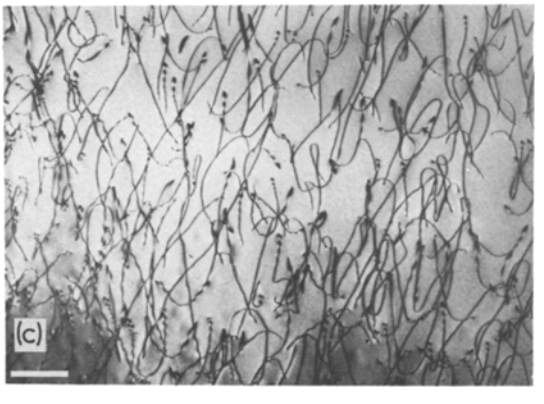

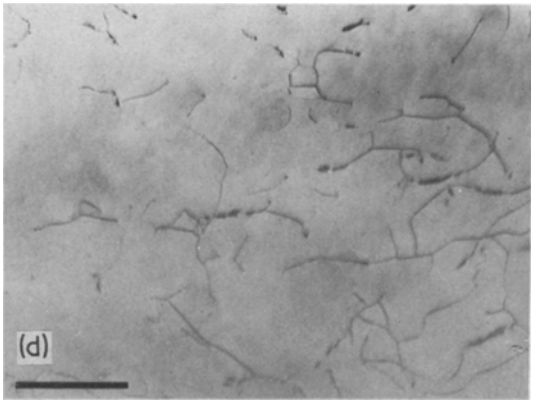

Figure 6 Typical dislocation structures inside the subgrain at the steady state for: (a) alpha iron crept to 20% strain at 700° C and 20 MN m^{-2}, bar ≡ 5 μm (from T. Iikubo, H. Oikawa and S. Karashima, private communication); (b) copper–10 at.% nickel crept to 16.8% strain at 600° C and 51.7 MN m^{-2}, bar ≡ 1 μm (from Jones and Sellars [113], courtesy of Institute of Metals); (c) aluminium–5.1 at.% magnesium crept to 5% strain, at 359° C and 48 MN m^{-2}, bar ≡ 1 μm (from Horiuchi and Otsuka [41], courtesy of Japan Institute of Metals); (d) Magnesium oxide, crept to 2.8% strain, at 1300° C and 60 MN m^{-2}, bar ≡ 1 μm (from Bilde-Sörensen [83], courtesy of Pergamon Press).

the subgrains characteristic of steady-state creep, except in class I alloys, are as follows. (1) Dislocations inside the subgrain have generally no strong directionality, although edge tendency in Mo [114] and screw tendency in Cu [141] were reported. (2) They form coarse networks (often called three-dimensional). (3) No pile-ups exist. (4) They sometimes form incomplete sub-boundaries.

Sub-boundaries are in some cases loosely knitted and in other cases well knitted depending upon the creep rate and temperature [131, 140]. Compared with b c c metals and Al (e.g. [107, 133]), Cu [139, 142] and Cu alloys [35, 44, 64] seem to have less tendency to form well-knitted sub-boundaries, suggesting the effect of the stacking fault energy on sub-boundary formation. Myshlyaov *et al.* [133] analysed regular dislocation networks and showed that non-equilibrium boundaries of different types dominate.

On the other hand, some alloys, mainly belonging to class I, have the following features. (1) Less tendency to form networks and sub-boundaries (Al–Mg [41, 136, 137], Cu–10 at. % Au [113], Fe–3.5 at. % Mo [152]). No sub-boundary formation until the later stages of steady-state creep has also been observed for W–5 wt % Re [165] and 20Cr–35Ni stainless steel [159] even though the stress exponent in these two alloys are 5.5 and 5, respectively. (2) Dislocations are very homogeneously distributed and in Al–Mg alloys they are mostly of edge character [41]. (3) They are smoothly curved, indicating the existence of a glide resistance on a very fine scale.

Recently, *in situ* observations of creep phenomena in a high voltage electron microscope (HVEM) using a high-temperature stage have been reported for Al–1% Mg [134, 135, 167]. Rather slow ($v \approx 10^{-2}\ \mu m\,sec^{-1}$) and continuous motion of dislocations was observed, but the total motion was not decomposed into glide and climb components. One remarkable observation shows that when a moving dislocation approaches a sub-boundary, its motion becomes retarded, starting from a distance of more than 1 μm away, and after passing through the sub-boundary the dislocation gradually recovers its velocity [135]. The authors attributed this phenomenon to the long range stress around the sub-boundary, which does not seem likely because in that case the velocity–distance relation should be asymmetric owing to the nature of internal stress. Although *in situ* experiments using HVEM have several problems, e.g. specimen size effect (although HVEM foils can be much thicker than TEM foils, they are still very thin relative to the subgrain size), effect of radiation damage, inhomogeneity of stress, etc., this technique has good potential to yield decisive information for the mechanism of steady state creep in the future.

3.4. Quantitative description of the dislocation structure

3.4.1. Misorientation of sub-boundaries

Electron-microscopic measurements show that the angle of misorientation of sub-boundaries range from 0.3 to 1° for Al [132], 0.3 to 1.2° for Fe [120], below 1° (average 0.3°) for W [164], 0.2 to 1.0° for an Al–Mg alloy [136] and 0.1 to 2.5° for a stainless steel [119]. These values are consistent with X-ray results for Al [99] and Fe [107, 168]. Misorientation angles for Ni were reported to be of the order of 1 to 2° by X-ray measurements [155] and for Cu to be as small as 0.1° or less by the X-ray (Berg–Barrett) method [169], by electron microscopy [142], and by etch-pit spacing [110]. The misorientation is larger for materials with higher stacking-fault

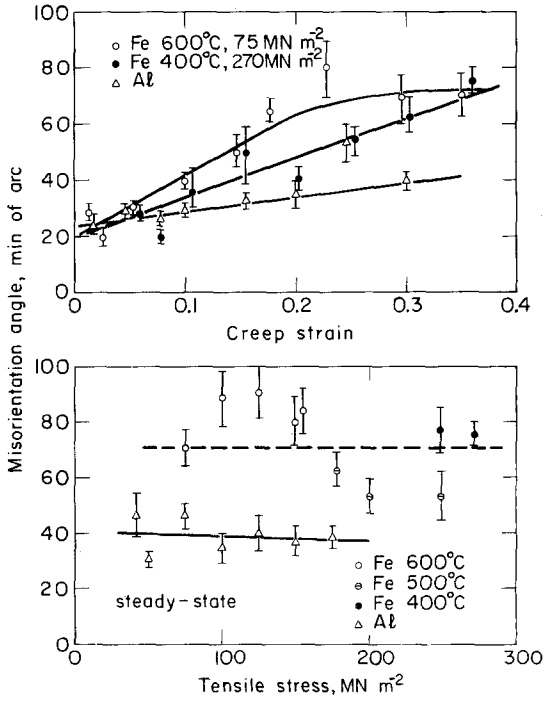

Figure 7 Angle of misorientation as a function of creep strain (upper) and of stress (lower) for Al and Fe (from [120] and [132]).

energy [170]. Misorientation angles increase gradually with increasing strain during transient creep [25, 99, 120, 132, 155, 168], and cease increasing when creep becomes steady [99, 120, 132, 168, 169]. Misorientation angles at steady-state creep are almost independent of stress and temperature [99, 120, 132]. Examples of change of misorientation with creep strain and stress for Al and Fe are shown in Fig. 7.

Considering that sub-boundaries may absorb glide dislocations, angles of misorientation may be expected to increase with strain. Substantially constant misorientation at steady-state creep is considered to be a result of the dynamic process of formation and annihilation of sub-boundaries mentioned above, since the impingement of two sub-boundaries always leads to lowering the misorientation angle, as pointed out by Exell and Warrington [99].

3.4.2. Subgrain size

The average subgrain size in steady-state creep has been measured as a function of stress, temperature and/or strain-rate [33, 86, 92, 93, 106, 108, 113, 115–120, 127, 129, 130, 132, 148, 151, 154, 155, 161, 171, 172], and it has been reported that the size is a function only of stress [92, 93, 106, 113, 119, 129, 164], except in a few exceptional cases [117, 120, 131]. The relation has usually been written as $d \propto \sigma^{-m}$, and as reviewed by others [5, 6, 8, 10, 13, 14, 19] $m \approx 1$, except in hot-working where Jonas *et al.* [12] report $m = 1.5$. In Table II, values of m for many materials given by different authors are tabulated together with the K value defined by

$$\tau = K\frac{\mu b}{d} \tag{11}$$

for cases of $m \approx 1$. In Fig. 8 the relations between d/b and τ/μ are shown only for single crystal specimens. In the evaluation of K (and α) in Table II and in the plot of Fig. 8 (and Fig. 10), the shear modulus μ is taken to be the shear modulus at the test temperature for the specific slip system of each material and τ to be the resolved shear stress for single crystal specimens, and $\sigma/2$ for poly-crystalline specimens. From Table II and Fig. 8, the typical relation which emerges is again that given by Equation 11 with the value of $K \approx 10$ for metals and $25 \approx 80$ for ionic crystals.

3.4.3. Dislocation density

Dislocation density inside the subgrain as measured by electron microscopy or the etch-pit method rapidly increases at the initial stage of transient creep but gradually decreases until the steady-state is reached (Al [173]; Cu [110, 111]; Fe [120, 148]; Fe–3% Si [106, 109]; Mo [114], stainless steel [162]; MgO [116], the ratio of maximum density to the density at the steady-state creep being about 2–5. However, the total density of dislocations including those composing

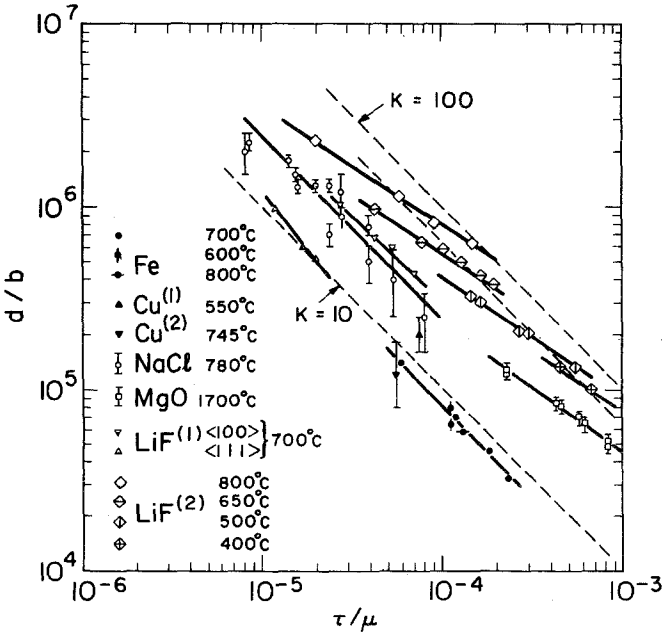

Figure 8 Relation between d/b and τ/μ at the steady-state of single crystal specimens of Fe [108], $Cu^{(1)}$ [110], $Cu^{(2)}$ [112], NaCl [115], MgO [116], $LiF^{(1)}$ [118] and $LiF^{(2)}$ [117].

TABLE II Constants of proportionality and exponents in structure–stress expressions. (OP, optical method; EP, etch-pit method; TEM, transmission electron microscopy). Symbols are defined by: $\rho \propto \tau^{l}$; $d \propto \tau^{-m}$; $\tau = \alpha \mu b \sqrt{\rho}$; $\tau = K\mu b/d$ (τ_0 in remarks is given by $\tau = \tau_0 + \alpha \mu b \sqrt{\rho}$, otherwise $\tau_0 = 0$. Shear modulus at test temperature for active slip system was used, $\tau = \sigma/2$ for polycrystals)

Material	Method	l	α	m	K	Remarks	Reference
Pure metals							
Al	TEM			1	~10	Including data of extrusion	[130]
	TEM	0.33		0.26		ρ depends on T	[132]
	EP	2	0.7			Single crystal, $\tau_0 < 0$	[173]
	TEM			~1	~13	Scattered data	[127]
	etching			0.7			[171]
	OP			0.7			[93]
	TEM			1	~13	Hot compression	[131]
Cu	EP	~1.5				By Strutt and Gifkins (cited in [110])	[110]
	EP	~2	2.6				[113]
	TEM	2	0.6	1	10	High temp. tensile test	[174]
Fe	TEM	~2	0.6			$\tau_0 < 0$	[147]
	TEM	0.95		0.4		d depends on T	[120]
	TEM, EP	1		1	8	Single crystal	[108]
	TEM	2	0.4				[146]
	TEM	~1					[148]
Ni	TEM	~2	~0.7	~1	5	Only two data points	[154]
W	EP, TEM			~1		No figure	[164]
Zr	TEM	~1					[151]
Alloys							
Al–Mg	TEM	~2	0.5			Mg; 3 at.% and 7 at.%	[41]
	TEM	~1				Mg; 5.5 at.%	[136]
	TEM	1.6	1.5			Mg; 5 at.%	[138]
Cu–Mo	TEM	1.7	0.35			Mo; 3.5 at.%	[152]
Cu–Ni	EP	~2	2.6			Ni; 10 at.%, $\tau_0 > 0$	[113]
Cu–Zn	TEM	1.4				Zn; 10 at.%	[145]
Fe–Cr	TEM	0.7				Cr; 20 at.%	[150]
Fe–Mo	EP, TEM	~1.5		~0.5		Mo; 4 wt%	[149]
Fe–3 wt% Si	EP	1.4				With (1 1 0) [0 0 1] texture	[25]
	EP			~2		Excluding region of lowest stress	[106]
	TEM	1					[151]
	EP	~2	1.4			Except low stress region	[84]
Carbon–steel	etching			1	7		[172]
Stainless	TEM	2	1.5			Type 316, $\tau_0 < 0$	[162]
steel	TEM	~2	0.4			20 Cr, 35 Ni	[156]
	TEM	1.4 ~ 2.0	~1.0	0.8	~7	19 Cr, 10 Ni	[119]
	TEM	~2	~1.5			20 Cr, 25 Ni Contain NbC precipitates	[157]
	TEM	~2	1.5	1	18	Slow tensile test $\tau_0 < 0$, 17 Cr, 12 Ni, 2 Mo	[161]
W–5 wt% Re	TEM	~2	0.4				[165]
W–Re	TEM	2.2	~0.5			Re 25% and 30% cited in [165]	

Table II continued

TABLE II continued.

Material	Method	l	α	m	K	Remarks	Reference
Ionic salts							
LiF	EP			1	10; 30	Single crystal, K depends on orientation	[118]
	EP	2	0.7–1.0	~1	40 ~ 80	For const. $\dot{\epsilon}$ } Mg-doped	[117]
		1		0.7		For const. T } single crystal	
MgO	EP, TEM	1.4		0.7		Single crystal	[116]
	TEM	~2	~1.0				[166]
	TEM	~2	~0.5			Data with large scatter	[83]
NaCl	EP			1	~25	Single crystal	[115]

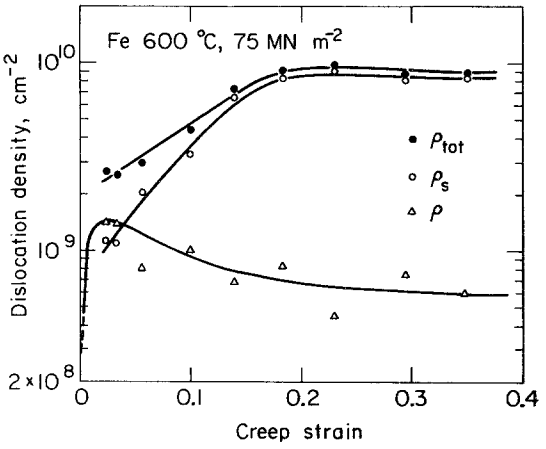

Figure 9 Change in dislocation density with creep strain for Fe. ρ is dislocation density inside subgrains as measured by transmission electron microscopy, ρ_s is that of dislocations composing subboundaries which is estimated from misorientation angle and subgrain size, and ρ_{tot} is the total density of $\rho + \rho_s$ (from [151]).

sub-boundaries has been estimated by Orlova and Čadek [151] to increase monotonically during transient creep and to level off at steady-state based on the data on misorientation and sub-boundary density. They showed that the ratio of density of dislocations inside subgrains to total density is only 0.1 for Al and Fe, and about 1.0 for Zn [151]. Fig. 9 shows the density change with strain for Fe. Dislocation density for Ni evaluated by X-ray methods was found to be lower in the transient creep region than in the steady-state creep region [115, 168]. In alloys where sub-boundary development is imperfect or altogether absent, dislocation density has been reported to increase monotonically with creep strain in the transient creep region [41, 138, 153, 159].

The dislocation density inside subgrains in steady-state creep has usually been correlated only with stress for many materials [25, 41, 83, 108, 110, 113, 117, 119, 120, 128, 147, 150, 156–159, 161, 164–166, 171, 173, 175], and only in a few papers [132, 151] has a correlation with temperature been sought. Stress dependence has in most cases been written as $\rho \propto \sigma^l$. The measured exponents l are listed in Table II. The exponent l is about 2 in the majority of cases, with the values of α defined by the following equation also being listed in Table II. The value α obtained from

$$\tau = \alpha\mu b\sqrt{\rho} \qquad (12)$$

is of the order of unity. Fig. 10 shows the relation

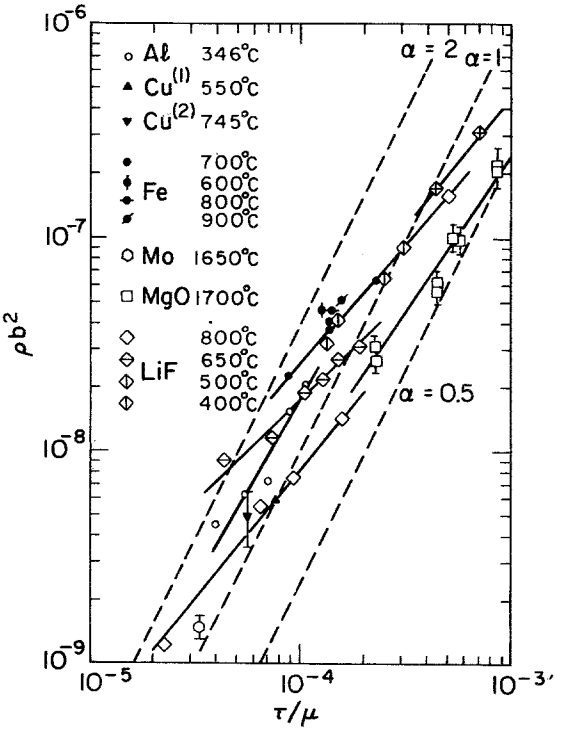

Figure 10 Relation between ρb^2 and τ/μ at the steady-state for single crystals of Al [173], $Cu^{(1)}$ [110], $Cu^{(2)}$ [111], Fe [108], Mo [114], MgO [116] and LiF [117]. ρ is dislocation density inside subgrains and τ the resolved shear stress.

between ρb^2 and τ/μ only for single crystal specimens.

Using the relation $\rho_{sb} = 3\theta/bd$, where θ is the average misorientation between subgrains, the total dislocation density at steady-state creep is expressed from Equations 11 and 12 as

$$\rho_{tot} = \rho_{sb} + \rho = \frac{\tau}{\mu b^2}\left(\frac{3\theta}{K} + \frac{\tau}{\alpha^2\mu}\right). \quad (13)$$

For the typical cases for metals, $\theta \simeq 10^{-2}$, $K = \tau d/\mu b \simeq 10$, $\alpha \simeq 1$. With these, Equation 13 is reduced to $\rho_{tot} = (\tau/\mu b^2)(0.003 + \tau/\mu)$. Thus, ρ_{sb} is found to be always larger than ρ under the usual creep conditions of $\tau/\mu \sim 10^{-4}$.

In recent years the distribution of segment lengths of dislocations forming three-dimensional networks has been measured by means of transmission electron microscopy for stainless steel [160, 176] and MgO [83]. Fig. 11 shows the distribution for MgO obtained by Bilde-Sörensen [83].

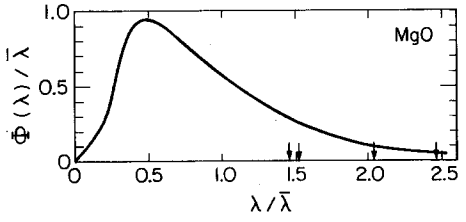

Figure 11 Average distribution function of segment lengths of dislocations at steady-state creep for four polycrystalline MgO specimens, $\bar{\lambda}$ is the average segment length. Arrows indicate the critical length of $\mu b/\tau$ for four specimens (from [83]).

4. Transient experiments

To measure the recovery rate under stress, to determine the effect of stress history on creep rate, and to check the Bailey–Orowan equation, stress change experiments have been performed by many researchers [35, 77, 113, 119, 147, 177–198]. Also, for the purpose of investigating the presence of internal stress, so-called stress- (or strain-) dip tests have been performed in recent years [39, 62, 143, 152, 199–210].

4.1. Bailey–Orowan equation

Assuming that the applied stress in creep is a function of time and strain,

$$d\sigma = \left(\frac{\partial\sigma}{\partial t}\right)_\epsilon dt + \left(\frac{\partial\sigma}{\partial\epsilon}\right)_t d\epsilon \equiv -r\,dt + h\,d\epsilon, \quad (14)$$

where r and h are defined as the recovery rate and the work-hardening rate, respectively. In constant stress creep where $d\sigma = 0$, Equation 14 leads to the Bailey–Orowan equation [211, 212]. Creep phenomena determined by this equation are called "recovery controlled" creep (see Section 5). An experiment to confirm this equation was performed by Mitra and McLean [185].

Experimentally, r is determined by measuring the incubation time for recommencement of creep strain after a stress reduction, i.e. $r = (\Delta\sigma/\Delta t)_{\Delta\sigma\to 0}$, see Fig. 12. The plateau region after a reduction of stress has earlier been investigated by Kennedy [178]. The work-hardening rate h has been determined by either one of two methods; one is the method by Mitra and McLean [154, 185], where h is approximated by the work-hardening rate at the creep stress in the stress–strain curve obtained at room temperature after the creep test; the other is the method first done by Ishida and McLean [147], where an instantaneous plastic strain increment $\Delta\epsilon$ after an instantaneous stress increase $\Delta\sigma$ is measured (see Fig. 12), and h is estimated by $h = (\Delta\sigma/\Delta\epsilon)_{\Delta\sigma\to 0}$. The latter method has been used most often.

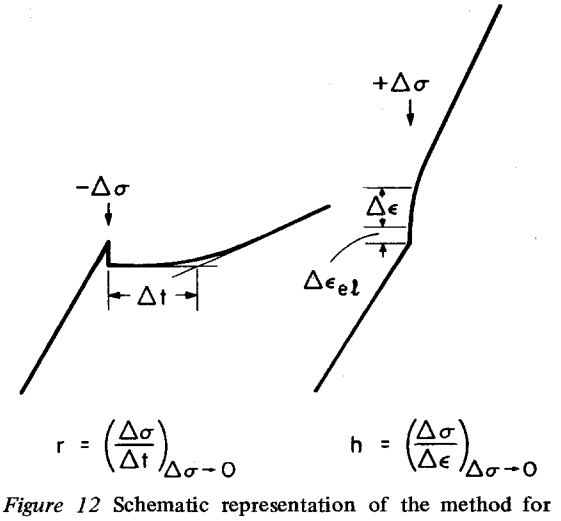

Figure 12 Schematic representation of the method for estimating recovery rate, r, and work-hardening rate, h, by means of the stress change method. $\Delta\epsilon_{el}$ means elastic strain increment resulting from stress increase.

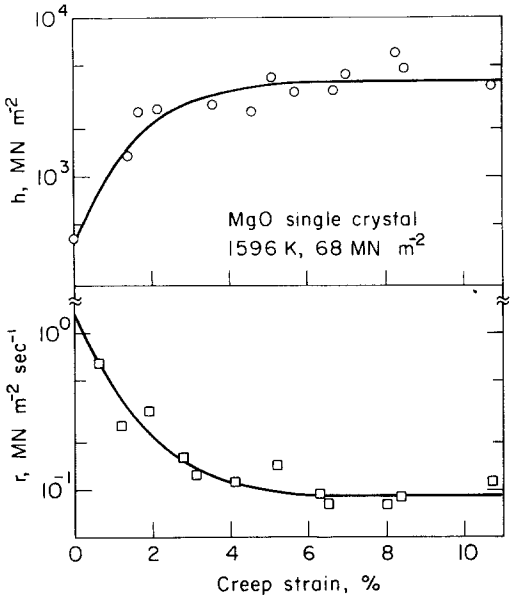

Figure 13 Change in recovery rate, r, and work-hardening rate, h, with creep strain for a MgO single crystal, estimated by the stress change method shown in Fig. 12 [197].

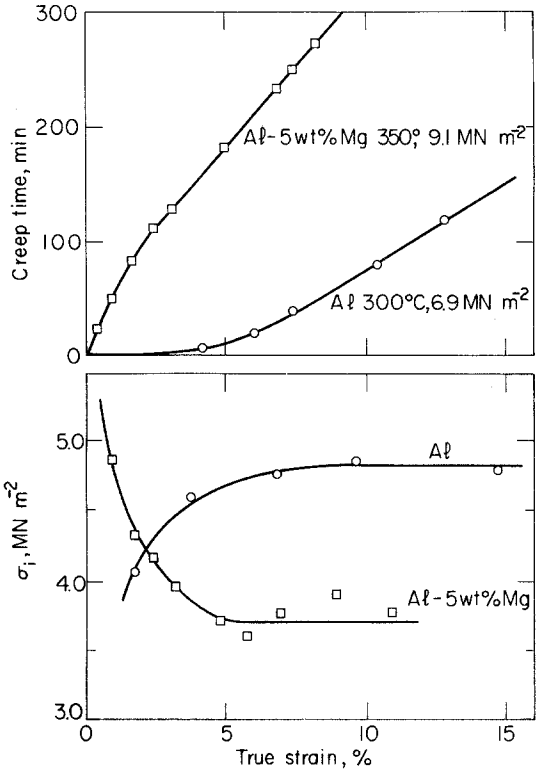

Figure 14 Creep curves (upper) and change of σ_i with strain (lower) for Al and Al–5 wt % Mg (from [39]).

The changes of r and h with creep time have been measured for α-brass [187], Ni–20% Cr [188], MgO [196, 197] and Cu–15% Al [35]. As shown in Fig. 13, r decreases and h increases in the transient creep region and both level off in steady-state, where h levels off earlier, in general, than r. In steady-state the value of r/h obtained in the above-mentioned manner has been compared with $\dot{\epsilon}_s$ for many materials; Ni and Al [185, 154], Fe [147], MgO [195, 197], Cu–15% Al [35], α-brass [187], Ni–Co alloys [77] and Ni–20% Cr [188]. All these results showed an order-of-magnitude agreement. Mitra and McLean [154] reported that the agreement is obtained also for the transient region after a stress reduction [154]. Stress dependence of r and h in the steady-state creep region are: $r \propto \sigma^3$ to $\sigma^{3.5}$ and $h \propto \sigma^{-1}$ to $\sigma^{-1.5}$ for Ni and Al [185]; $r \propto \dot{\epsilon}_s$ and $h \simeq$ constant for Cu–16% Al [35]. It should be noted that the measured h is always unusually high and of the order of shear modulus (see a table in [194]), this makes the method for determining h suspect.

As will be mentioned later, the creep behaviour after a stress change is complex and the above experiments cannot be interpreted in a simple way. Fig. 14 shows the change in σ_i, the internal stress, (see Section 4.2) with strain for Al and Al–5 wt % Mg, together with creep curves. The decrease of the observed internal stress with strain in the transient creep region in Al–5 wt % Mg where the curvature is positive is difficult to be rationalized considering the continuous increase of the dislocation density in this alloy as mentioned in Section 3.

4.2. Internal stress

After an instantaneous stress reduction, close examination shows that if the stress is kept constant, the subsequent strain-rate is positive or negative, and if the specimen length is kept constant, the stress begins to decrease (relaxation) or increase, depending upon the amount of stress reduction. The former type of experiment is called the stress-dip test, while the latter is called the strain-dip test. On the basis of the simple concept of internal stress, the critical stress in these tests where the subsequent initial strain-rate is zero has been regarded as an internal stress as was done by Gibbs [199]. These techniques have been applied to many materials to estimate the internal stress (Mg [199], Cu and its alloys [143, 204, 205], Fe and its alloys [62, 153, 175, 200, 202, 209,

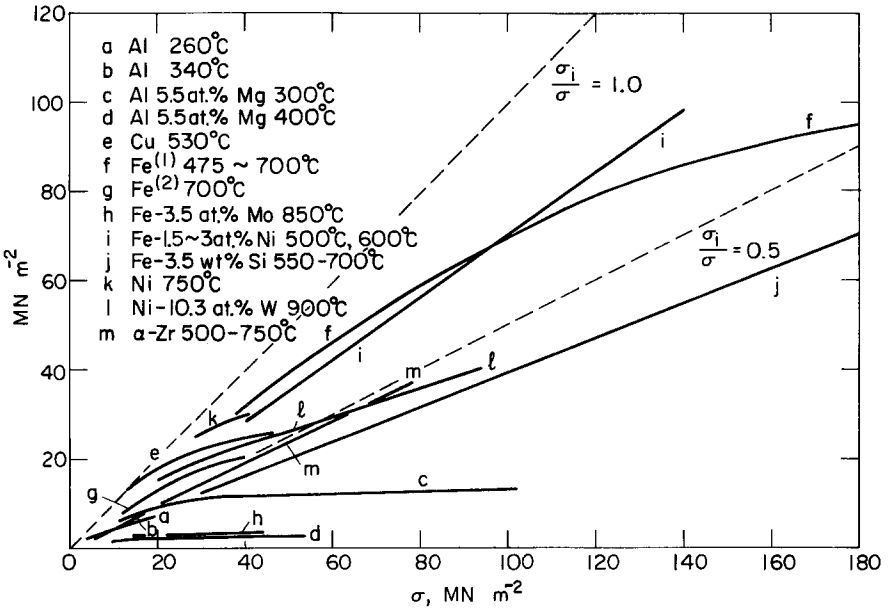

Figure 15 σ_i versus σ relations for various materials (Al [203], Al–5.5 at.% Mg [208], Cu [143], $Fe^{(1)}$ [175], $Fe^{(2)}$ [209], Fe–3.5 at.% Mo [209], Fe–1.5 to 3 at.% Ni [62] Fe–3.5 at.% Si [202], Ni [209], Ni–10.3 at.% W [209] and α–Zr [206]).

210], Al and its alloys [39, 60, 203, 207, 208], Zr [206], and Ni and its alloys [63, 209]. The internal stress σ_i obtained in this manner increases or decreases with strain and levels off at steady-state creep [39, 210]). Fig. 14 shows the change in σ_i with strain for Al and Al–5 wt % Mg (class I alloy), together with creep curves. The ratio of internal stress to the stress for steady-state creep is generally a function of stress and temperature. Fig. 15 shows examples for many materials. In some cases, σ_i is proportional to stress with a proportionality constant of 0.4 (for Fe–3.5 % Si [202]) and 0.5 (for α-Zr [206]), but in other cases the ratio σ_i/σ is a decreasing function of stress. Oikawa and Karashima reported that the values of the ratio for alloys do not necessarily correlate with the classes to which they belong [209]. As stated in the next section, a simple interpretation of this experiment is not easy, although the origin of the internal stress has been discussed by many authors [45, 58, 119, 204, 214, 215].

4.3. Complex behaviour after stress change

Real creep behaviour after stress change is not so simple as was assumed in previous sections. A simple interpretation of the incubation period is that it is the time taken for the three-dimensional network to grow in size corresponding to the new stress [213]. The strain-rate resumed after an incubation time in the stress dip test, however, does not correspond to the steady-state creep rate at that reduced stress [77, 113, 154, 181, 192, 197]. It has been shown that the transient region before the final steady-state consists of two stages as shown in Fig. 16 [77, 192, 197, 204]. Mitra and McLean showed for Ni that during 0.5% strain

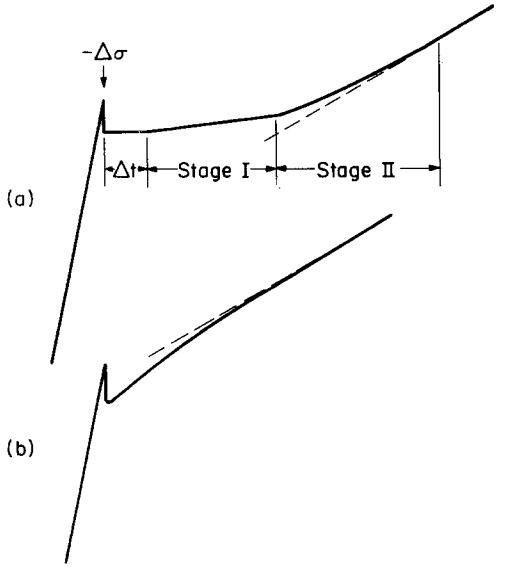

Figure 16 Schematic drawing of the transient behaviour of the creep curve after a stress-drop at steady-state for pure metals (a) and for class I alloys (b).

increment after the stress reduction, no detectable change in dislocation density occurs [154]. They interpreted that the strain increment might be brought about by the motion of a small fraction of long dislocation segments composing the three-dimensional network. Birch and Wilshire interpreted that during stage I (Fig. 16) only network growth occurs and in stage II subgrain growth takes place as well as continued network growth until the final steady-stage structure is attained [197]. For class I alloys (Al–Mg [183], Cu–Au [113]), on the other hand, the strain-rate after the stress reduction is faster than the steady-state value as schematically shown in Fig. 16.

The stress dependence of the initial creep rate following the incubation time was measured for Ni and Al by Mitra and McLean [154]. As shown in Fig. 17, the stress exponent doubles compared with that for steady-state creep. Considering that little change in structure occurs during this measurement, the above dependence may be taken as that for a constant structure test. Constant structure tests by this stress reduction method have first been performed by Sherby *et al.* for Al [180], and later for stainless steel by Cuddy [119]. Using the same technique, Robinson *et al.* [216–218] showed the relationship among $\dot{\epsilon}$ d and σ of the form $\dot{\epsilon} \propto d^P(\sigma/E)^N$; $P = 2$, $N = 7$ for W and $P = 3$, $N = 7$ for Al. However, another structure parameter ρ is always related to d at steady-state and the above relation must have been obtained for various values of ρ: consequently, it cannot simply be interpreted to indicate the effect of subgrain size on the creep rate.

As seen in dip-tests for internal stress measurements, the creep curve during the incubation period is, in general, not exactly constant. Lubahn as early as 1953 [179] measured creep recovery strain ϵ_r after partly or fully unloading a commercial steel and found that ϵ_r increases linearly with the amount of stress decrement. On the other hand, forward strain (during a standard unloading period) is of the form $\epsilon_f \propto \sigma^n$ $(n \gg 1)$. From these facts, Lubahn explained the finite limiting reduced stress below which no substantial positive creep strain is observed. He also suggested ϵ_r to be of anelastic nature. Bayce *et al.* [183] also interpreted the transient creep curve after a stress reduction in the primary creep region of A to be composed of recovery creep and forward creep. Henderson and Snedden [219] measured re-

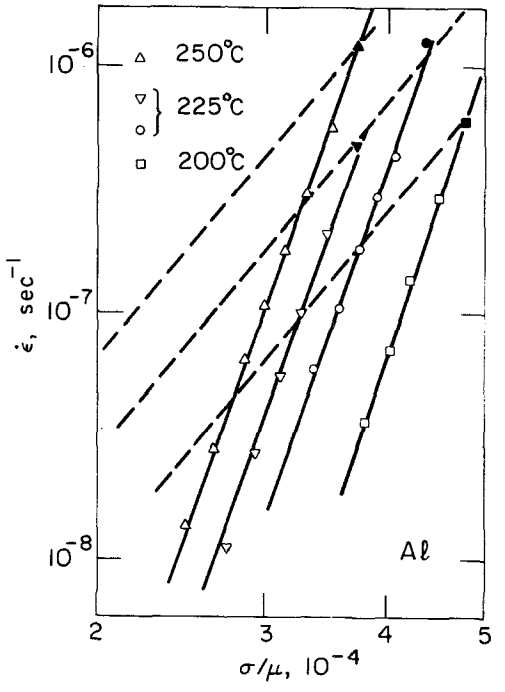

Figure 17 Stress dependence of the initial creep rate after various amounts of stress reduction at steady-state creep of Al. Solid marks indicate initial states. Dashed lines are the stress dependence of ϵ_s for each temperature (from [154]).

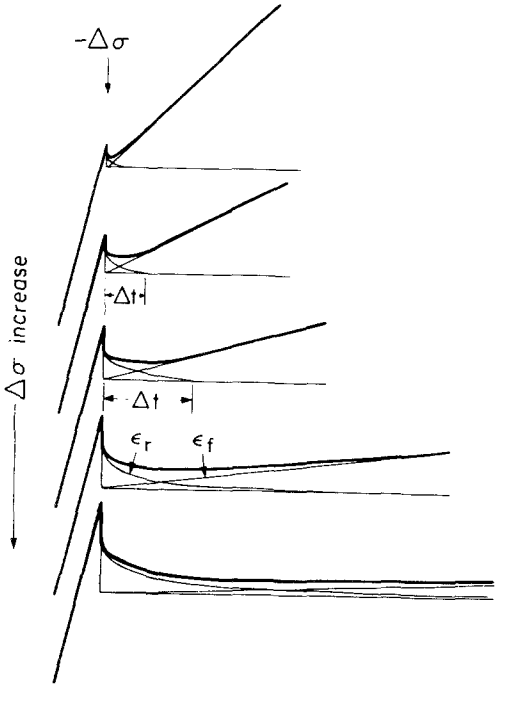

Figure 18 A series of transient curves after various amounts of stress drops. Creep strain after a stress drop is decomposed into two components, recovery strain, ϵ_r, and forward creep strain, ϵ_f (see [194]).

covery strain of Cu and discussed its relation to the transient creep strain. These experiments showed that ϵ_r after unloading is of the order of 10^{-4} to 10^{-3}. Davies and Wilshire showed that the instantaneous contraction of the specimen accompanying a stress reduction contains a considerable plastic recovery component in addition to the elastic contraction [201]. In Fig. 18, transient curves after various amounts of stress reduction are schematically drawn. Lloyd and McElroy showed recently that the incubation time following a stress reduction can be interpreted to be the time during which forward strain is approximately equal to the anelastic recovery strain which is linear with the stress reduction $\Delta\sigma$, see Fig. 18 [194]. According to this interpretation, $\Delta t \simeq \epsilon_r/\dot{\epsilon}_f$ and thus $r = \Delta\sigma/\Delta t \simeq \Delta\sigma\ (\dot{\epsilon}_f/\epsilon_r)$, which implies that r no longer means a simple recovery rate. They also showed that the observed equality, $\dot{\epsilon} = r/h$, can be rationalized by assuming that the observed strain increment after a stress increase is due to anelastic strain, i.e. $h = \Delta\sigma/\epsilon_r$. Such an interpretation leads to the further conclusion that σ_i obtained in the dip test does not correspond to the internal stress in a static sense but it corresponds to the stress at which the initial anelastic strain-rate is equal to the forward strain-rate.

In stress reversal experiments an acceleration of the creep rate has been reported for Pb [177], Al [220] and stainless steel [191]. Wilson interpreted the Bauschinger effect, as well as the recovery creep after unloading to be an anelastic phenomenon resulting from back motion of dislocations [191].

As stated previously, sub-boundaries are mobile under the action of the applied stress and their motion contributes to a considerable fraction of the total strain. As a consequence, in addition to the back motion of bowed-out dislocations [191, 194], straightening of bulged sub-boundaries after an instantaneous stress drop is considered to be an important contribution to the anelastic strain.

In summary, simple interpretations of the results of transients in creep experiments discussed in Sections 4.1 and 4.2 are generally of doubtful validity.

5. Proposed models for steady-state creep

5.1. Grain-boundary sliding

Sliding of grains along boundaries in creep has been known for a long time. Many investigators have specifically measured the amount of sliding along grain boundaries during creep [221], and have tried to estimate the contribution of such sliding to the total creep strain [222]. Such estimates have always ranged from very small fractions to very very large fractions. That grain-boundary sliding is not an independent mechanism producing steady creep strain has been pointed out by a number of investigators [223]. More recently, Raj and Ashby [224] presented mechanistic models showing that in steady-state creep grain-boundary sliding must be integrally connected with intra-crystalline creep deformation. The effect of coupled grain-boundary sliding and intra-crystalline creep on the overall creep law has been studied by Hart [225] and by Crossman and Ashby [226]. The latter point out that both when the boundaries slide freely (transmitting no shear traction) and when they do not slide at all there is no effect of the boundaries on the overall creep law, even though in the first case, the stress and strain-rate distribution in the polycrystal is highly inhomogeneous. The largest effect of the sliding boundaries on the overall creep law occurs when the average relative sliding displacement rate $\dot{u}$ across the boundary is about equal to the relative creep shear displacement across the grain, i.e. when:

$$\dot{u} = w\frac{\bar{\tau}}{\eta_B} = d\left[A\left(\frac{\bar{\tau}}{\mu}\right)^n\right] \tag{15}$$

where w and η_B are the effective thickness of the grain boundary and its effective shear viscosity, while A is a constant and $\bar{\tau}$ is the average local shear stress. Other terms have their previously defined meaning. It can be shown readily that at the transition from free sliding to no sliding where the above condition holds, the average shear stress $\bar{\tau}$ and the intra-crystalline shear strain-rates $\dot{\gamma}_{ig}$ respectively

$$\bar{\tau} = \mu\left(\frac{w}{d}\frac{\mu}{A\eta_B}\right)^{1/n-1} \tag{16}$$

$$\dot{\gamma}_{ig} = A\left(\frac{w}{d}\frac{\mu}{A\eta_B}\right)^{(n/n-1)} \tag{17}$$

Furthermore, at the transition where the effect of the grain-boundary sliding is maximum, the effective creep exponent n' drops down to a value of

$$n' = \left(\frac{n+1}{2}\right) \tag{18}$$

5.2. Phenomenological description of steady-state creep

In steady-state creep it is necessary that some condition for internal structural balance be satisfied. It must be noted that in its statement, the Bailey–Orowan equation does not mean a steady-state, but only a state of constant stress. At a given external condition, the creep rate is determined by the microstructure parameters S_i, such as the dislocation density, i.e.

$$\dot{\epsilon} = f(S_i \sigma, T). \tag{19}$$

On the other hand, since the microstructure changes with time (due to recovery) and strain (due to work-hardening), the steady-state condition under a constant stress is:

$$dS_i = \left(\frac{\partial S_i}{\partial t}\right)_\epsilon dt + \left(\frac{\partial S_i}{\partial \epsilon}\right)_t d\epsilon = 0, \tag{20}$$

which gives:

$$\dot{\epsilon} = -\frac{(\partial S_i/\partial t)_\epsilon}{(\partial S_i/\partial \epsilon)_t} \tag{21}$$

Therefore, a steady strain-rate and a steady-state structure are realized when Equations 19 and 21 are satisfied simultaneously. This argument was first advanced by Cottrell and Aytekin [29], who regarded S_i as an average internal stress. Recently, similar but more refined treatments have been given by Gittus [227, 228], Gibbs [229], Kocks [230], and Grant [231], using hypothetical or empirical functional forms for S_i. Generally, both Equations 19 and 20 can involve different rate processes. As a result, the observed activation process of $\dot{\epsilon}_s$ could be of a complex form. Experiments show, however, that the observed activation energy is very close to Q_{sd}, which seems to indicate that $\dot{\epsilon}_s$ is governed by a simple activation process. Thus, it is natural to consider the following two extreme cases:

(1) The deformation mechanism is itself of athermal nature and $(\partial S_i/\partial t)_\epsilon$ is governed by self-diffusion. In this case, Equation 19 is written as $f(S_i, \sigma) = 0$. Hence Equation 21 is reduced to the Bailey–Orowan equation, i.e.

$$\dot{\epsilon} = -\frac{(\partial S_i/\partial t)_\epsilon}{(\partial S_i/\partial \epsilon)_t} = \frac{-(\partial \sigma/\partial t)_\epsilon (dS_i/d\sigma)_\epsilon}{(\partial \sigma/\partial \epsilon)_t (dS_i/d\sigma)_t} = \frac{-(\partial \sigma/\partial t)_\epsilon}{(\partial \sigma/\partial \epsilon)_t} = \frac{r}{h}. \tag{22}$$

It should be noted, in this context, that the structure need not depend only on a single parameter which is a function of stress, because if this were so, a constant stress would always lead to a constant structure, and hence, to a constant strain-rate. In this respect, Alden's theory of plastic flow [232] is different, where two structure parameters, a density parameter and an arrangement parameter, are introduced and the strain-rate is formulated taking the recovery of both parameters into account.

(2) Another case is that the structure parameter, S_i, is determined only by ϵ under a constant σ, independently of $\dot{\epsilon}$ so that S_i is not related by Equation 21. The activation process in creep deformation is that which is involved in glide (Equation 19) with the activation energy of Q_{sd}.

The former type of creep is called "recovery controlled" and the latter "glide controlled". In the following, we will survey, in historical order, the proposed models based on dislocation processes.

5.3. Models for steady-state creep

5.3.1. Climb-controlled glide model

Weertman first formulated a model where the creep rate is controlled by the escape rate, by means of climb, of leading dislocations piled up at obstacles [49], and later modified the original theory [10]. Using a model of multipole formation by Hazzledine, Weertman calculated the annihilation rate of dipoles and obtained $\dot{\epsilon}_s \propto \mu D/kT \cdot (\sigma/\mu)^{4.5}$ under the assumption of constant number of dislocation sources. The successful feature of his theory is in the correct stress exponent, in contrast to other theories in which an exponent larger than 4 has not been obtainable. This model, however, does not seem to be supported by direct observations, as already discussed by many researchers.

5.3.2. Viscous glide model

This model is applicable only to solid solution alloys, where the viscous glide of dislocations, dragging solute atmosphere, governs the deformation. Weertman deduced a third power relation from the linear viscous motion of piled-up dislocations [50], which again is not supported by electron micrographs of dislocation structures in alloys. Friedel treated the dislocation line–tension-assisted diffusion of pinning atoms, and obtained a simple form of $\dot{\epsilon}_s \simeq 2\rho D\sigma b^3/kT$

[233]. Using an empirical relation of $\sigma \simeq \mu b\sqrt{\rho}$, Bird *et al.* showed a good agreement between the above equation and experiments (see Fig. 10 of [14]). The agreement, however, appears to be fortuitous because Friedel's theory is essentially based on a dilute solid solution, although the result is independent of concentration. In any case, linear viscous motion of dislocations and the 2nd power dependence of ρ on stress lead to the dependence of the strain-rate on the third power of the stress. The relation of $\rho \propto \sigma^2$ at the steady-state follows from a balance equation such as Equation 21. Horiuchi and Otsuka [41] obtained the above result from the equation of $\dot{\epsilon}_s = \rho b v$ (where $v \propto \sigma$), and the balance equation between the multiplication rate of dislocations (which is assumed to be proportional to $\dot{\epsilon}_s$) and the annihilation rate by climb (which is assumed to be proportional to the density of dislocations times the reciprocal of their spacing). Their assumptions, however, are questionable, e.g. the annihilation time of a trapped pair should be proportional roughly to the inverse square of the spacing.

5.3.3 Jog-dragging screw model

The motion of a jogged screw dislocation was discussed by Mott 25 years ago [234] and was applied later to the temperature dependence of the flow stress of pure metals in the high temperature region by Hirsch and Warrington [235]. Dorn and Mote [5] formulated, in more detail, the thermally activated motion of a jogged screw dislocation under stress under the condition of equilibrium vacancy concentration near jogs. Barrett and Nix [55] calculated the dislocation velocity under the condition of steady flow of vacancies to and from jogs. Revisions and modifications of the theory have been done several times [236–240]. These treatments all give a σ–v relation for a single dislocation (at low stress $\sigma \propto v$). The mobile dislocation density, ρ_m, must be determined from another condition. A reasonable derivation of a σ–ρ_m relationship to give the observed stress exponent of $\dot{\epsilon}_s$ has, however, not been given. Furthermore, owing to the statistical variation of jog spacings, line density of jogs previously formed must always decrease due to the conservative motion of jogs on screw dislocations [241] and thus the motion of a jogged screw dislocation is essentially unstable, unless the thermal production rate of jogs is larger than their rate of annihilation. A simple calculation shows readily that the thermal equilibrium concentration under stress of jogs on a straight screw dislocation is negligibly small under the usual test condition.

5.3.4. Network growth model

On the basis of Friedel's network recovery theory [233], Mitra and McLean [185] deduced a recovery rate with a third power of stress dependence, in agreement with their stress-dip test. From the network growth rate of $d\bar{\lambda}/dt \propto \bar{\lambda}^{-1}$ by Friedel and the assumption $\sigma \propto \bar{\lambda}^{-1}$, where $\bar{\lambda}$ is the average network spacing,

$$r = -\left(\frac{\partial \sigma}{\partial t}\right)_\epsilon = -\left(\frac{\partial \bar{\lambda}}{\partial t}\right)_\epsilon \cdot \frac{d\sigma}{d\bar{\lambda}} \propto \frac{1}{\bar{\lambda}^3}. \quad (23)$$

Combined with the experimental fact of $h \propto \sigma^{-1.5}$ (see Section 4.1), they explained the observed stress exponent. Lagneborg later refined this theory [242, 243]. Gittus also formulated a creep equation along the same lines [244, 245]. Considering that the exact meaning of the dip-test is not clear, as mentioned in Section 4.3, qualitative agreement between this model and the transient experiment does not necessarily signify validity of this model.

If the creep stress were uniquely related to $\bar{\lambda}$, then after a reduction of stress, no further creep strain would appear until $\bar{\lambda}$ increases to the value corresponding to the reduced stress, which is not in agreement with experimental facts (see Section 4.3). Thus, the distribution of dislocation segment lengths and its change with time have been used rather than the average value to explain experimental results on the creep transient in the dip test [154, 157, 194]. In these treatments, only a fractional number of segments whose lengths grow to the critical length contribute to deformation. Such a process must be labelled as exhaustion hardening, rather than barrier hardening. Lagneborg *et al.* [246] recently performed a detailed statistical treatment on the change of the distribution function of λ by recovery and compared with experimental data.

5.3.5. Diffusional model

Nabarro assumed a special type of regular array of edge dislocations with two sets of Burgers vectors, their spacing being determined by the applied stress. He calculated the creep rate due to a steady climb motion of these dislocations (with no accompanying glide) and obtained a third

power law for the stress dependence [247]. Dupouy modified this theory taking the effect of periodic internal stresses into consideration, and showed that the stress exponent can then be very large [248]. These models bring up the point that there is no reliable means by which the various contributions of glide and climb to the overall creep strain can be determined. The reacted network configuration of Nabarro is also not free of problems since neighbouring segments with different Burgers vectors must climb in different directions which leads to the destruction of the network.

5.3.6. Sub-boundary recovery model

Based on the easy climb motion of knitted dislocations on sub-boundaries, Lindroos and Miekk-oja proposed a model that the creep rate is controlled by successive annihilation of two groups of dislocations with opposite signs that are climbing up and down along the sub-boundary after gliding from the opposite sides of the adjoining subgrains to knit it [249]. This model also requires dislocation pile-ups against the sub-boundary, which are not observed.

Blum [250] proposed a model that the sub-boundary regions with a high dislocation density (cell boundary) act as dislocation barriers and that the recovery rate of dislocations in this area controls the deformation rate. This model cannot be applied to the case of well-knitted sub-boundaries.

5.4. Concluding remarks

It may be concluded that class I alloys are controlled by linear viscous motion of dislocations. The present authors worked out a theory where the structure balance due to production and annihilation of dislocations was treated in detail [251]. For other materials, it may be said at the present time, that existing theories or models are not fully successful in explaining experiments. Among them, only the network growth model seems to be compatible with the results of direct observation. However, the following points are worth making:

(1) Friedel's network recovery theory used in deriving Equation 23 does not take the effect of applied stress into account. In reality, however, there is a well-known effect that the cold-worked materials recover much faster under stress than under no stress (see for Al [252–254]), indicating an important role of dynamic recovery. Kocks [255] recently produced arguments for the existence of a saturation stress in the constant strain-rate tests over the whole temperature range, and explained it by a dynamic recovery process.

(2) As shown below, the steady-state creep rate in the network growth theory should always be proportional approximately to σ^3 as long as the principle of similitude holds, i.e. the dislocation behaviour is identical when the length dimension is normalized by $\bar{\lambda}$ which is inversely proportional to σ and the time scale is appropriately normalized. From dimensional arguments, $-(\partial\lambda/\partial\epsilon)_t \propto \lambda^2$ – note that $\delta\epsilon = \boldsymbol{b}x$(area swept by dislocations)/(unit volume) $\propto \lambda^{-1}$ – which corresponds to a constant work-hardening rate. The rate of growth of networks, on the other hand, takes place by climb motion due to interaction between dislocations, the velocity of the ith dislocation being given by the form $v_i \propto (\ln \bar{\lambda}/\boldsymbol{b})\Sigma\alpha_{ij} r_{ij}^{-1}$, where r_{ij} is the distance between ith and jth dislocation and α_{ij} is a geometric factor. The factor $\ln \bar{\lambda}/\boldsymbol{b}$ comes in as the outer cut-off radius of the diffusion controlled climbing process. Thus, the rate of growth of network spacing is given by the form of $(\partial\bar{\lambda}/\partial t)_\epsilon \propto \ln(\bar{\lambda}/\boldsymbol{b})/\bar{\lambda}$. Hence,

$$\dot{\epsilon} = -\frac{(\partial\bar{\lambda}/\partial t)_\epsilon}{(\partial\bar{\lambda}/\partial\epsilon)_t} \propto \ln(\bar{\lambda}/\boldsymbol{b})/\bar{\lambda}^3 \propto \xi\sigma^3, \quad (24)$$

where ξ is an insensitive function of σ. Therefore, to explain the observed stress exponent, we must make some assumption that violates similitude, i.e. either the work-hardening rate is not a constant value but a decreasing function of stress [11, 185, 244] or the recovery rate is a more sensitive function of stress than the similitude principle shows [35]. These are, however, difficult to be rationalized within the framework of the network growth model.

(3) The role of sub-boundaries are not yet clear. The stress-subgrain relation of Equation 11 itself has never been explained except by the theory of cell formation of Holt [256], which gives only the initial conditions of instability of networks. The mobile nature of sub-boundaries under stress mentioned in Section 3.1. is important in the dynamic recovery because their motion results in the scavenging of network dislocations. Also, if the new sub-boundaries are formed by a recovery

process of network dislocations due to some instability effect, as in the Holt theory, then the subgrain growth due to sub-boundary migration serves as a large recovery because ρ_s is an order of magnitude larger than ρ as mentioned in Section 3. The possible recovery due to sub-boundary motion has already been pointed out by others [114, 184, 257].

At any rate, to verify which recovery process is the main, controlling process, it appears to be necessary to perform continuous observations of structures by various techniques.

References

1. A. H. SULLY, *Prog. Mater. Sci.* 6 (1956) 135.
2. H. CONRAD, in "Mechanical Behaviour of Materials at Elevated Temperatures, edited by J. E. Dorn (McGraw-Hill, New York, 1961) p. 149.
3. G. SCHOECK, *ibid* p. 79.
4. D. MCLEAN, *Met. Rev.* 7 (1962) 481.
5. J. E. DORN and J. D. MOTE, in "High Temperature Structure and Materials", edited by A. M. Freudenthal, B. A. Boley and H. Liebowitz (Pergamon Press, Oxford, 1964) p. 95.
6. F. GAROFALO, "Fundamentals of Creep and Creep-Rupture in Metals" (MacMillan, New York, 1965).
7. D. MCLEAN, *Rep. Prog. Phys.* 29 (1966) 1.
8. O. D. SHERBY and P. M. BURKE, *Prog. Mater. Sci.* 13 (1967) 325.
9. L. M. T. HOPKIN, *Prog. Appl. Mater. Res.* 7 (1967) 33.
10. J. WEERTMAN, *Trans. ASM* 61 (1968) 680.
11. D. MCLEAN, *Trans. Met. Soc. AIME* 242 (1968) 1193.
12. J. J. JONAS, C. M. SELLARS and W. J. McG. TEGART, *Met. Rev.* 14 (1969) 1.
13. A. K. MUKHERJEE, J. E. BIRD and J. E. DORN, *Trans. ASM* 62 (1969) 155.
14. J. E. BIRD, A. K. MUKHERJEE and J. E. DORN, in "Quantitative Relation Between Properties and Microstructure", edited by D. G. Brandon and A. Rosen (Israel Univ. Press, Jerusalem, 1969) p. 255.
15. F. R. N. NABARRO, in "Report of a Conference on the Strength of Solids" (The Physical Society, London, 1948) p. 75.
16. C. HERRING, *J. Appl. Phys.* 21 (1950) 437.
17. R. L. COBLE, *ibid* 34 (1963) 1679.
18. J. HARPER and J. E. DORN, *Acta Met.* 5 (1957) 654.
19. G. J. DAVIES, J. W. EDINGTON, C. P. CUTLER and K. A. PADMANABHAN, *J. Mater. Sci.* 5 (1970) 1091.
20. C. R. BARRETT, J. L. LYTTON and O. D. SHERBY, *Trans. Met. Soc. AIME* 239 (1967) 170.
21. D. MCLEAN, *J. Inst. Metals* 80 (1951–2) 507.
22. B. FAZAN, O. D. SHERBY and J. E. DORN, *Trans. Met. Soc. AIME* 200 (1954) 919.
23. D. MCLEAN and M. H. FARMER, *J. Inst. Metals* 85 (1956–57) 41.
24. H. BRUNNER and N. J. GRANT, *Trans. Met. Soc. AIME* 215 (1959) 48.
25. J. L. LYTTON, C. R. BARRETT and O. D. SHERBY, *ibid* 233 (1965) 1399.
26. H. C. CHANG and N. J. GRANT, *ibid* 197 (1953) 1175.
27. *Idem, J. Inst. Metals* 82 (1953–54) 229.
28. E. N. DA C. ANDRADE, *Proc. Roy. Soc. (London)* A84 (1911) 1.
29. A. H. COTTRELL and V. AYTEKIN, *J. Inst. Metals* 77 (1950) 389.
30. J. B. CONWAY and M. J. MULLIKIN, *Trans. Met. Soc. AIME* 236 (1966) 1496.
31. P. G. MCVETTY, *Mech. Eng.* 56 (1934) 149.
32. G. A. WEBSTER, A. P. D. COX and J. E. DORN, *Metal Sci. J.* 3 (1969) 221.
33. F. GAROFALO, C. RICHMOND, W. F. DOMIS and F. VON GEMMINGEN, Joint International Conference on Creep, 1963 (Inst. Mech. Engineers, London, 1965) p. 1–31.
34. W. J. EVANS and B. WILSHIRE, *Trans. Met. Soc. AIME* 242 (1968) 1303.
35. *Idem, Metal Sci. J.* 4 (1970) 89.
36. J. C. M. LI, *Acta Met.* 11 (1963) 1269.
37. W. G. JOHNSTON and J. J. GILMAN, *J. Appl. Phys.* 30 (1959) 129.
38. H. LAKS, C. D. WISEMAN, O. D. SHERBY and J. E. DORN, *J. Appl. Mech.* 24 (1957) 207.
39. C. N. AHLQUIST and W. D. NIX, *Acta Met.* 19 (1971) 373.
40. T. IIKUBO, H. OIKAWA and S. KARASHIMA, *Scripta Met.* 5 (1971) 837.
41. R. HORIUCHI and M. OTSUKA, *Trans. Jap. Inst. Metals* 13 (1972) 284.
42. W. J. EVANS and B. WILSHIRE, *Met. Trans.* 1 (1970) 2133.
43. R. A. MENEZES and W. D. NIX, *Acta Met.* 19 (1971) 645.
44. W. A. COGHLAN, R. A. MENEZES and W. D. NIX, *Phil. Mag.* 23 (1971) 1515.
45. T. HASEGAWA' Y. IKEUCHI and S. KARASHIMA, *Metal Sci. J.* 6 (1972) 78.
46. H. ALEXANDER and P. HAASEN, *Sol. Stat. Phys.* 22 (1968) 27.
47. B. ANCKER, T. H. HAZLETT and E. R. PARKER, *Trans. Met. Soc. AIME* 27 (1956) 333.
48. J. WEERTMAN, *J. Appl. Phys.* 26 (1955) 1213.
49. *Idem, ibid* 28 (1957) 362.
50. *Idem, ibid* 28 (1957) 1185.
51. F. GAROFALO, *Trans. Met. Soc. AIME* 227 (1963) 351.
52. C. M. SELLARS and W. J. Mc G. TEGART, *Mem Sci. Rev. Metal.* 63 (1966) 731.
53. J. J. JONAS, D. R. AXELRAD and J. L. UVIRA *Trans. Jap. Inst. Metals Suppl.* 9 (1968) 257.
54. J. L. UVIRA and J. J. JONAS, *Trans. Met. Soc. AIME* 242 (1968) 1619.
55. C. R. BARRETT and W. D. NIX, *Acta Met.* 13 (1965) 1247.
56. Y. ISHIDA, C. Y. CHANG and J. E. DORN, *Trans. Met. Soc AIME* 236 (1966) 964
57. N. BALASUBRAMANIAN and J. C. M. LI, *J. Mater.*

Sci. **5** (1970) 434.
58. J. J. JONAS, *Acta Met.* **17** (1969) 397.
59. F. A. NICHOLS, *Mater Sci. Eng.* **8** (1971) 108.
60. K. KUCHAŘOVÁ and J. ČADEK, *Phys. Stat. Sol. (a)* **6** (1971) 33.
61. B. REPPICH and G. STREB, *ibid* **15** (1973) 77.
62. L. J. CUDDY and J. C. RALEY, *Acta Met.* **21** (1973) 427.
63. H. OIKAWA, T. KATO and S. KARASHIMA, *Trans. Jap. Inst. Metals* **14** (1973) 389.
64. T. HASEGAWA, S. KARASHIMA and Y. IKEUCHI, *Acta Met.* **21** (1973) 887.
65. J. E. DORN, in "Creep and Recovery" (ASM, Cleveland, Ohio, 1957) p. 255.
66. O. D. SHERBY and J. L. LYTTON, *Trans. Met. Soc. AIME* **206** (1956) 928.
67. O. D. SHERBY, *ibid* **212** (1958) 708.
68. C. R. BARRETT, A. J. ARDELL and O. D. SHERBY, *ibid* **230** (1964) 200.
69. S. L. ROBINSON, P. M. BURKE and O. D. SHERBY, *Phil. Mag.* **29** (1974) 423.
70. J. WEERTMAN, *Trans. Met. Soc. AIME* **218** (1960) 207.
71. C. M. SELLARS and A. G. QUARRELL, *J. Inst. Metals* **90** (1961–62) 329.
72. F. A. MOHAMED and G. LANGDON, *Acta. Met.* **22** (1974) 779.
73. W. R. CANNON and O. D. SHERBY, *Met. Trans.* **1** (1970) 1030.
74. K. L. MURTY, *Phil. Mag.* **29** (1974) 429.
75. F. A. MOHAMED and T. G. LANGDON, *Met. Trans.* **6A** (1975) 927.
76. C. R. BARRETT and O. D. SHERBY, *Trans. Met. Soc. AIME* **233** (1965) 1116.
77. C. K. L. DAVIES, P. W. DAVIES and B. WILSHIRE, *Phil. Mag.* **12** (1965) 827.
78. R. M. BONESTEEL and O. D. SHERBY, *Acta Met.* **14** (1966) 385.
79. J. HEDWORTH and G. POLLARD, *Metal Sci. J.* **5** (1971) 41.
80. H. OIKAWA and S. KARASHIMA, *Scripta Met.* **5** (1971) 909.
81. F. A. MOHAMED and T. G. LANGDON, *J. Appl. Phys.* **45** (1974) 1965.
82. T. G. LANGDON and J. A. PASK, *Acta Met.* **18** (1970) 505.
83. J. B. BILDE-SORENSEN, *ibid* **21** (1973) 1495.
84. C. H. M. JENKINS and G. A. MELLOR, *J. Iron Steel Inst.* **132** (1935) 179.
85. G. R. WILMS and W. A. WOOD, *J. Inst. Metals* **75** (1948–49) 693.
86. W. A. WOOD and W. A. RACHINGER, *ibid* **76** (1949–50) 237.
87. W. A. WOOD and R. F. SCRUTTON, *ibid* **77** (1950) 423.
88. G. B. GREENNOUGH and E. M. SMITH, *ibid* **77** (1950) 435.
89. E. C. CALNAN and B. D. BURNS, *ibid* **77** (1950) 445.
90. W. A. WOOD, G. R. WILMS and W. A. RACHINGER, *ibid* **79** (1951) 159.
91. W. A. RACHINGER, *ibid* **80** (1951–52) 415.
92. I. S. SERVI and N. J. GRANT, *Trans. Met. Soc. AIME* **191** (1951) 917.
93. I. S. SERVI, J. T. NORTON and N. J. GRANT, *Trans. AIME (J. Metals)* **194** (1952) 965.
94. J. W. KELLY and R. C. GIFKINS, *J. Inst. Metals* **82** (1953–54) 475.
95. A. M. GERVAIS, J. T. NORTON and N. J. GRANT, *Trans. Met. Soc. AIME* **197** (1953) 1166.
96. G. D. GEMMELL and N. J. GRANT, *Trans. AIME (J. Metals)* **209** (1957) 417.
97. H. C. CHANG and N. J. GRANT, *Trans, AIME (J. Metals)* **194** (1952) 619.
98. N. J. GRANT and A. CHANDHURI, in: "Creep and Recovery" (ASM, Cleveland, Ohio, 1957) p. 284.
99. S. F. EXELL and D. H. WARRINGTON, *Phil. Mag.* **26** (1972) 1121.
100. J. WASHBURN and E. R. PARKER, *J. Metals* **4** (1952) 1076.
101. C. H. LI, E. H. EDWARDS, J. WASHBURN and E. R. PARKER, *Acta Met.* **1** (1953) 223.
102. D. W. BAINBRIDGE, C. H. LI and E. H. EDWARDS, *ibid* **2** (1954) 322.
103. A. HIGASHI and N. SAKAI, *J. Phys. Soc. Japan* **16** (1961) 2359.
104. S. KARASHIMA, T. HASEGAWA and M. YOKOTA, *J. Jap. Inst. Metals* **32** (1968) 218.
105. H. GLEITER, *Phil. Mag.* **20** (1969) 821.
106. C. R. BARRETT, W. D. NIX and O. D. SHERBY, *Trans. Amer. Soc. Metals* **59** (1966) 3.
107. F. GAROFALO, L. ZWELL, A. S. KEH and S. WEISSMANN, *Acta Met.* **9** (1961) 721.
108. S. KARASHIMA, T. IIKUBO and H. OIKAWA, *Trans. Jap. Inst. Metals* **13** (1972) 176.
109. A. I. MAKHATILOVA, L. V. MINIMA, YE. F. SIDOKHIN and L. M. UTEVSKIY, *Phys. Met. Metallogr.* **36** (6) (1973) 150.
110. V. P. GUPTA and P. R. STRUTT, *Canad. J. Phys.* **45** (1967) 1213.
111. T. HASEGAWA, R. HASEGAWA and S. KARASHIMA, *Trans. Jap. Inst. Metals* **11** (1970) 101.
112. T. HASEGAWA, S. KARASHIMA, and R. HASEGAWA, *Met. Trans.* **2** (1971) 1449.
113. B. L. JONES and C. M. SELLARS, *Metal Sci. J.* **4** (1970) 96.
114. A. H. CLAUER, B. A. WILCOX and J. P. HIRTH, *Acta Met.* **18** (1970) 381.
115. J. P. POIRIER, *Phil. Mag.* **26** (1972) 713.
116. W. HÜTHER and B. REPPICH, *ibid* **28** (1973) 363.
117. G. STREB and B. REPPICH, *Phys. Stat. Sol. (a)* **16** (1973) 493.
118. D. R. CROPPER and J. A. PASK, *Phil. Mag.* **27** (1973) 1105.
119. L. J. CUDDY, *Met. Trans.* **1** (1970) 395.
120. A. ORLOVÁ, M. PAHUTOVÁ and J. ČADEK, *Phil. Mag.* **25** (1972) 865.
121. T. HASEGAWA, H. SATO and S. KARASHIMA, *Trans. Jap. Inst. Metals* **11** (1970) 94.
122. A. ORLOVÁ and J. ČADEK, *Phil. Mag.* **21** (1970) 509.
123. A. ORLOVÁ, R. FIEDLER and J. ČADEK, *ibid* **24** (1971) 733.
124. B. REPPICH and W. HÜTHER, *ibid* **30** (1974) 1009.

125. A. H. CLAUER, B. A. WILCOX and J. P. HIRTH, *Acta Met.* **18** (1970) 367.
126. J. C. M. LI, *J. Appl. Phys.* **33** (1962) 2958.
127. E. G. BELKIN, N. N. DEMIKHOVSKAYA, I. E. KUROV and M. M. MYSHLYAEV, *Phys. Stat. Sol. (a)* **16** (1973) 425.
128. F. H. HAMMAD and W. D. NIX, *Trans. Amer. Soc. Metals* **59** (1966) 95
129. M. M. MYSHLYAEV, *Sov. Phys.-Solid State* **9** (1967) 937.
130. H. J. McQUEEN, W. A. WONG and J. J. JONAS, *Canad. J. Phys.* **45** (1967) 1225.
131. H. J. McQUEEN and J. E. HOCKETT, *Met. Trans.* **1** (1970) 2997.
132. A. ORLOVÁ, Z. TOBOLOVÁ and J. ČADEK, *Phil. Mag.* **26** (1972) 1263.
133. M. M. MYSHLYAEV, S. S. OLEVSKII and S. K. MAKSIMOV, *Phys. Stat. Sol. (a)* **15** (1973) 391.
134. K. F. HALE, M. HENDERSON BROWN and Y. ISHIDA, Proceedings of the 5th European Congress on Electron Microscopy, Manchester (Institute of Physics, London, 1972) p.350.
135. M. HENDERSON BROWN and K. F. HALE, in "High Voltage Electron Microscopy" (Proc. 3rd Intern. Conf.), edited by P. R. SWANN, C. J.HUMPHREYS and M. J. GORINGE (Academic Press, New York, 1974) p. 206.
136. A. ORLOVÁ and J. ČADEK, *Z. Metallkde.* **65** (1974) 200.
137. N. MATSUNO, H. OIKAWA and S. KARASHIMA *J. Jap. Inst. Metals* (in Japanese) **38** (1974) 1071.
138. H. OIKAWA, N. MATSUNO and S. KARASHIMA, *Metal Sci.* **9** (1975) 209.
139. P. FELTHAM and R. A. SINCLAIR, *J. Inst. Metals* **91** (1962–63) 235.
140. C. R. BARRETT, *Acta Met.* **13** (1965) 1088.
141. T. HASEGAWA and S. KARASHIMA, *Met. Trans.* **1** (1970) 1052.
142. T. HASEGAWA, H. SATA and S. KARASHIMA, *Trans. Jap. Inst. Metals* **11** (1970) 231.
143. D. J. LLOYD and J. D. EMBURY, *Metal Sci. J.* **4** (1970) 6.
144. A. ORLOVÁ, M. PAHUTOVÁ and J. ČADEK, *Phil. Mag.* **23** (1971) 303.
145. T. HOSTINSKÝ and J. ČADEK, *Phil. Mag.* **31** (1975) 1177.
146. D. McLEAN and K. F. HALE, in "Structural Processes in Creep" (Iron Steel Inst., Rep. No. 70, 1961) p. 19. (Cited in [9].)
147. Y. ISHIDA and D. McLEAN *J. Iron Steel Inst.* **205** (1967) 88.
148. S. KARASHIMA, T. IIKUBO, T. WATANABE and H. OIKAWA, *Trans. Jap. Inst. Metals* **12** (1971) 369.
149. A. FUCHS and B. ILSCHNER, *Acta Met.* **17** (1969) 701.
150. N. IGATA, K. MIYAHARA and T. TAOKA, *Jernkont. Ann.* **155** (1971) 373.
151. A. ORLOVÁ and J. ČADEK, *Phil Mag.* **28** (1973) 891.
152. H. OIKAWA, M. MAEDA and S. KARASHIMA, *J. Jap. Inst. Metals* (in Japanese) **37** (1973) 599.
153. M. MAEDA, H. OIKAWA and S. KARASHIMA, *Scripta Met.* **8** (1974) 183.
154. S. K. MITRA and D. McLEAN, *Metal Sci. J.* **1** (1967) 192.
155. V. V. LEVITIN and V. K. ORZHITSKAYA, *Phys. Met. Metallogr.* **30** (4) (1970) 172.
156. R. LAGNEBORG, *Metal Sci. J.* **3** (1969) 18.
157. K. R. WILLIAMS and I. R. McLAUCHLIN, *J. Mater. Sci.* **5** (1970) 1063.
158. L. ROHLIN, *Jernkont. Ann.* **155** (1971) 381.
159. B. MODÉER and R. LAGNEBORG, *ibid* **155** (1971) 363.
160. A. ODÉN, E. LIND and R. LAGNEBORG, *ibid* **155** (1971) 386.
161. D. J. MITCHEL, J. MOTEFF and A. J. LOVELL, *Acta Met.* **21** (1973) 1269.
162. V. K. SIKKA, H. NAHM and J. MOTEFF, *Mater. Sci. Engr.* **20** (1975) 55.
163. R. R. VANDERVOORT and W. L. BARMORE, *Trans. Met. Soc. AIME*, **245** (1969) 825.
164. R. C. RAU, S. F. BARTØRAM and P. N. FLAGELLA, *Trans. Amer. Soc. Metals* **61** (1968) 647.
165. R. R. VANDERVOORT, *Met. Trans.* **1** (1970) 857.
166. J. B. BILDE-SÖRENSEN, *J. Amer. Ceram. Soc.* **55** (1972) 606.
167. M. HENDERSON BROWN, K. F. HALE and R. LAGNEBORG, *Scripta Met.* **7** (1973) 1275.
168. V. V. LEVITIN, V. I. BABENKO and A. L. ZLATSIN, *Phys. Met. Metallogr.* **35** (4) (1973) 139.
169. S. KARASHIMA, H. OIKAWA and T. HASEGAWA, *J. Jap. Inst. Metals* (in Japanese) **31** (1967) 782.
170. G. YA. KOZYRSKIY, P. N. OKRAINETS and V. K. PISHCHAK, *Phys. Met. Metallogr.* **34** (3) (1972) 151.
171. C. R. BARRETT, E. C. MUEHLEISEN and W. D. NIX, *Mater. Sci. Eng.* **10** (1972) 33.
172. A. GOLDBERG, *J. Iron Steel Inst.* **204** (1966) 268.
173. S. DAILY and C. N. AHLQUIST, *Scripta Met.* **6** (1972) 95.
174. M. R. STAKER and D. L. HOLT, *Acta Met.* **20** (1972) 569.
175. M. PAHUTOVÁ, A. ORLOVÁ, K. KUCHAROVÁ and J. ČADEK, *Phil. Mag.* **28** (1973) 1099.
176. A. ODÉN, E. LIND and R. LAGNEBORG, in "Creep Strength in Steel and High-Temperature Alloys" (The Metals Society, London, 1974) p. 60.
177. E. N. da C. ANDRADE and K. H. JOLLIFFE, *Proc. Roy. Soc. (London)* **A213** (1952) 3.
178. A. J. KENNEDY, *Brit. J. Appl. Phys.* **4** (1953) 225.
179. J. D. LUBAHN, *Trans. Amer. Soc. Metals* **45** (1953) 787.
180. O. D. SHERBY, R. FRENKEL, J. NADEAU and J. E. DORN, *Trans. AIME (J. Metals)* **200** (1954) 275.
181. O. D. SHERBY, T. A. TROZERA and J. E. DORN, *Proc. Amer. Soc. Test. Mater.* **56** (1956) 789.
182. W. D. LUDEMANN, L. A. SHEPARD and J. E. DORN, *Trans. Met. Soc. AIME* **218** (1960) 923.
183. A. E. BAYCE, W. D. LUDEMANN, L. A. SHEPARD and J. E. DORN, *Trans. Amer. Soc. Metals* **52** (1960) 451.

184. L. RAYMOND and J. E. DORN, *Trans. Met. Soc AIME* **230** (1964) 560.
185. S. K. MITRA and D. McLEAN, *Proc. Roy. Soc.* **295** (1966) 288.
186. T. WATANABE and S. KARASHIMA, *Trans. Jap. Inst. Metals, Suppl.* **9** (1968) 242.
187. W. J. EVANS and B. WILSHIRE, *Trans. Met. Soc. AIME* **242** (1968) 2514.
188. D. SIDEY and B. WILSHIRE, *Metal Sci. J.* **3** (1969) 56.
189. C. R. BARRETT, C. N. AHLQUIST and W. D. NIX, *Metal Sci. J.* **4** (1970) 41.
190. T. WATANABE and S. KARASHIMA, *ibid* **4** (1970) 52.
191. E. G. WILSON, *J. Sheffield Univ. Met. Soc.* **11** (1972) 21.
192. P. W. DAVIES, G. NELMES, K. R. WILLIAMS and B. WILSHIRE, *Metal Sci. J.* **7** (1973) 87.
193. T. B. GIBBONS, J. S. HERD, L. N. McCARTNEY and D. McLEAN, *Metal Sci. J.* **7** (1973) 196.
194. G. J. LLOYD and R. J. McELROY, *Acta Met.* **22** (1974) 339.
195. J. M. BIRCH and B. WILSHIRE, *J. Mater. Sci.* **9** (1974) 794.
196. *Idem, ibid* **9** (1974) 871.
197. *Idem, Phil. Mag.* **30** (1974) 1023.
198. C. M. YOUNG, S. L. ROBINSON and O. D. SHERBY, *Acta Met.* **23** (1975) 633.
199. G. B. GIBBS, *Phil. Mag.* **13** (1966) 317.
200. A. A. SOLOMON and W. D. NIX, *Acta Met.* **18** (1970) 863.
201. P. W. DAVIES and B. WILSHIRE, *Scripta Met.* **5** (1971) 475.
202. M. PAHUTOVÁ, T. HOSTINSKÝ and J. ČADEK, *Acta Met.* **20** (1972) 693.
203. Z. TOBOLOVÁ and J. ČADEK, *Phil. Mag.* **26** (1972) 1419.
204. P. W. DAVIES, G. NELMES, K. R. WILLIAMS and B. WILSHIRE, *Metal Sci. J.* **7** (1973) 87.
205. S. KIKUCHI, M. KAJITANI, T. ENJO and M. ADACHI, *J. Jap. Inst. Metals* (in Japanese) **37** (1973) 228.
206. M. PAHUTOVÁ and J. ČADEK, *Mater. Sci. Eng.* **11** (1973) 151.
207. H. OIKAWA, J. KARIYA and S. KARASHIMA, *Metal Sci. J.* **8** (1974) 106.
208. K. KUCHAROVÁ, I. SAXL and J. ČADEK, *Acta Met.* **22** (1974) 465.
209. H. OIKAWA and S. KARASHIMA, *Met. Trans.* **5** (1974) 1179.
210. S. TAIRA, M. INOHARA and M. FUJINO, *Trans. Iron Steel Inst. Japan* **14** (1974) 331.
211. R. W. BAILEY, *J. Inst. Met.* **35** (1926) 27.
212. E. OROWAN, *J. West Scotl. Iron Steel Inst.* **54** (1946–47) 45.
213. B. BURTON, *Metal Sci. J.* **9** (1975) 297.
214. D. J. LLOYD and J. D. EMBURY, *Met. Sci. J.* **4** (1970) 6.
215. A. ORLOVÁ and J. ČADEK, *Z. Metallkd.* **65** (1974) 55.
216. S. L. ROBINSON and O. D. SHERBY, *Acta Met.* **17** (1969) 109.
217. S. L. ROBINSON, C. M. YOUNG and O. D. SHERBY, *J. Mater. Sci.* **9** (1974) 341.
218. C. M. YOUNG, S. L. ROBINSON and O. D. SHERBY, *Acta Met.* **23** (1975) 633.
219. J. HENDERSON and J. D. SNEDDEN, *J. Mech. Engnr. Sci.* **10** (1968) 24.
220. M. KITAGAWA, C. E. JASKE and J. MORROW, in "Fatigue at High Temperature", ASTM, STP 459 (ASTM, Philadelphia, 1969) p. 100.
221. H. BRUNNER and N. J. GRANT, *Trans. Met. Soc. AIME* **218** (1960) 122.
222. A. J. KENNEDY, "Processes of Creep and Fatigue in Metals" (Oliver and Boyd, Edinburgh, 1962).
223. F. A. McCLINTOCK and A. S. ARGON, "Mechanical Behaviour of Materials" (Addison Wesley, Reading, Mass., 1966) p. 632.
224. R. RAJ and M. F. ASHBY, *Met. Trans.* **2** (1971) 113.
225. E. W. HART, *Acta Met.* **15** (1967) 1545.
226. F. W. CROSSMAN and M. F. ASHBY, *ibid* **23** (1975) 425.
227. J. H. GITTUS, *Phil. Mag.* **21** (1970) 495.
228. *Idem, ibid* **23** (1971) 1281.
229. G. B. GIBBS, *ibid* **23** (1971) 771.
230. U. F. KOCKS, in "Rate Processes in Plastic Deformation of Materials", edited by J. C. M. Li and A. K. Mukherjee (ASM, Metals Park, Ohio, 1975) p. 356.
231. C. GRANT, *J. Mech. Eng. Sci.* **16** (1974) 205.
232. T. H. ALDEN, *Phil. Mag.* **25** (1972) 785.
233. J. FRIEDEL, "Dislocations" (Addison Wesley, Reading, Mass., 1964) pp. 409, 239.
234. N. F. MOTT, *Phil. Mag.* **43** (1952) 1151.
235. P. B. HIRSCH and D. H. WARRINGTON, *ibid* **6** (1961) 735.
236. W. D. NIX, *Acta Met.* **15** (1967) 1079.
237. V. V. LEVITIN, *Phys. Met. Metallogr.* **32** (4) (1971) 190.
238. T. WATANABE and S. KARASHIMA, *Trans. Jap. Inst. Metals* **11** (1970) 159.
239. B. A. VERSHOK and A. L. ROYTBURD, *Phys. Met. Metallogr.* **35** (1973) 32.
240. M. MALU and J. K. TIEN, *Acta Met.* **22** (1974) 145.
241. N. LOUAT and C. A. JOHNSON, *Phil. Mag.* **7** (1962) 2051.
242. R. LAGNEBORG, *Metal. Sci. J.* **3** (1969) 161.
243. R. LAGNEBORG, *ibid* **6** (1972) 127.
244. J. H. GITTUS, *Acta Met.* **22** (1974) 789.
245. *Idem, ibid* **22** (1974) 1179.
246. R. LAGNEBORG, B. H. FORSÉN and J. WIBERG, in "Creep Strength in Steel and High-Temperature Alloys" (The Metals Society, London, 1974) p. 1.
247. F. R. N. NABARRO, *Phil. Mag.* **16** (1967) 231.
248. J. M. DUPOUY, *ibid* **22** (1970) 205.
249. V. K. LINDROOS and H. M. MIEKK-OJA, *ibid* **17** (1968) 119.
250. W. BLUM, *Phys. Stat. Sol. (b)* **45** (1971) 561.
251. S. TAKEUCHI and A. S. ARGON, *Acta Met.* in press.
252. W. A. WOOD and J. W. SUITER, *J. Inst. Metals* **80** (1951–52) 501.
253. O. D. SHERBY, A. GOLDBERG and J. E. DORN, *Trans. Amer. Soc. Metals* **46** (1954) 680.
254. K. O. BOGARDUS, M. S. HUNTER, M. HOLT and

G. R. FRANK, Jun., in "Joint International Conference on Creep, 1963" (Inst. Mech. Eng. London, 1965) p. 1–17.
255. U. F. KOCKS, *J. Eng. Mats. Technol.*, **98** (1976) 76.
256. D. L. HOLT, *J. Appl. Phys.* **41** (1970) 3197.
257. W. D. LUDEMANN, L. A. SHEPARD and J. E. DORN, *Trans. Met. Soc. AIME* **218** (1960) 923.
Received 22 January and accepted 6 February 1976.